

RESEARCH

Open Access



# Cerium oxide and barium sulfate nanoparticle inhalation affects gene expression in alveolar epithelial cells type II

Daniela Schwotzer<sup>\*</sup> , Monika Niehof, Dirk Schaudien, Heiko Kock, Tanja Hansen, Clemens Dasenbrock and Otto Creutzenberg

## Abstract

**Background:** Understanding the molecular mechanisms of nanomaterial interacting with cellular systems is important for appropriate risk assessment. The identification of early biomarkers for potential (sub-)chronic effects of nanoparticles provides a promising approach towards cost-intensive and animal consuming long-term studies. As part of a 90-day inhalation toxicity study with CeO<sub>2</sub> NM-212 and BaSO<sub>4</sub> NM-220 the present investigations on gene expression and immunohistochemistry should reveal details on underlying mechanisms of pulmonary effects. The role of alveolar epithelial cells type II (AELI cells) is focused since its contribution to defense against inhaled particles and potentially resulting adverse effects is assumed. Low dose levels should help to specify particle-related events, including inflammation and oxidative stress.

**Results:** Rats were exposed to clean air, 0.1, 0.3, 1.0, and 3.0 mg/m<sup>3</sup> CeO<sub>2</sub> NM-212 or 50.0 mg/m<sup>3</sup> BaSO<sub>4</sub> NM-220 and the expression of 391 genes was analyzed in AELI cells after one, 28 and 90 days exposure. A total number of 34 genes was regulated, most of them related to inflammatory mediators. Marked changes in gene expression were measured for Ccl2, Ccl7, Ccl17, Ccl22, Ccl3, Ccl4, Il-1 $\alpha$ , Il-1 $\beta$ , and Il-1rn (inflammation), Lpo and Noxo1 (oxidative stress), and Mmp12 (inflammation/lung cancer). Genes related to genotoxicity and apoptosis did not display marked regulation. Although gene expression was less affected by BaSO<sub>4</sub> compared to CeO<sub>2</sub> the gene pattern showed great overlap. Gene expression was further analyzed in liver and kidney tissue showing inflammatory responses in both organs and marked downregulation of oxidative stress related genes in the kidney. Increases in the amount of Ce were measured in liver but not in kidney tissue. Investigation of selected genes on protein level revealed increased Ccl2 in bronchoalveolar lavage of exposed animals and increased Lpo and Mmp12 in the alveolar epithelia.

**Conclusion:** AELI cells contribute to CeO<sub>2</sub> nanoparticle caused inflammatory and oxidative stress reactions in the respiratory tract by the release of related mediators. Effects of BaSO<sub>4</sub> exposure are low. However, overlap between both substances were detected and support identification of potential early biomarkers for nanoparticle effects on the respiratory system. Signs for long-term effects need to be further evaluated by comparison to a respective exposure setting.

**Keywords:** Nanoparticles, Gene expression, CeO<sub>2</sub>, BaSO<sub>4</sub>, Inhalation, Biomarkers, Alveolar epithelial cells type II, Inflammation, Oxidative stress

## Background

Nanotechnologies and -materials are of great interest for product development and since several years

its application is getting more popular. For safe use by manufacturers and consumers assessment of toxicity and adverse health effects is required. The present investigations are part of a comprehensive project on the toxicity and carcinogenicity of nanoparticles with nano-CeO<sub>2</sub> as representative material in different concentrations covering the low to moderate dose range (0.1, 0.3, 1.0,

\*Correspondence: daniela.schwotzer@item.fraunhofer.de  
Fraunhofer Institute for Toxicology and Experimental Medicine ITEM,  
Nikolai-Fuchs-Straße 1, 30625 Hannover, Germany

3.0 mg/m<sup>3</sup>), and nano-BaSO<sub>4</sub> at one high concentration (50.0 mg/m<sup>3</sup>) for comparison to a non-toxic and safe material. The project is funded by the German Federal Ministry of Education and Research (03X0149) and should provide supporting data on a combined chronic inhalation toxicity and carcinogenicity study with cerium oxide and barium sulfate nanoparticles [NANoREG (81|0661|10|170)]. The automotive industry uses CeO<sub>2</sub> nanoparticles in catalyzers and as fuel additive because of the material's catalytic properties. Due to its chemical inertness, barium sulfate is used in multiple applications e.g. as filler in the biomedical sector. The nanoparticles were examined in a 90-day inhalation toxicity study with obligatory endpoints according to OECD TG 413 [1]. To identify early biomarkers for long-term effects of nanoparticles and investigate potential mechanisms of action, highly sensitive methods (gene expression analysis, immunohistochemistry) were further included in the project and are described in the present article.

Depending on their size and the striving to form agglomerates, nanoparticles penetrate different parts of the respiratory tract and likely end up in the alveolar space. They potentially react with cellular systems and induce inflammatory reactions or other molecular events. They further might pass the air–blood-barrier and translocate to extra-pulmonary organs. One major mechanism for the elimination of particles from the respiratory tract is the uptake by alveolar macrophages and clearance via the mucociliary escalator or the lymphatic system. However, the alveolar space consists of further cell types involved in host defense and lung function maintenance. Alveolar epithelial type II (AEII) cells are responsible for production and recycling of lung surfactant, play a role in turnover of the alveolar epithelia, and bear the ability to transform into alveolar epithelial type I (AEI) cells (e.g. for replacement of damaged cells). It has early been reviewed that AEII cells are an important component of the respiratory defense system against foreign material, including nanoparticles [2]. They produce and secrete a variety of factors, like surfactant proteins and chemokines to recruit macrophages and induce inflammatory processes for substance elimination [2–6]. It has been shown that carbon black nanoparticles, but not fine or nano-TiO<sub>2</sub>, or fine carbon black stimulate AEII cells to release factors for macrophage migration *in vitro* [7]. Furthermore, AEII cells and not macrophages are assumed to be the main producers of neutrophil attracting chemokines in the early inflammatory response to carbon nanoparticles administered via intratracheal instillation [8]. AEII cells might also internalize nanomaterial via different mechanisms, including the route of surfactant recycling [9–13]. *In vivo* studies on gold nanoparticles demonstrate the presence of the

respective nanomaterial in lamellar bodies of AEII cells or the lung lining fluid [14, 15].

The presence of nanomaterial in the lung can cause chronic inflammatory reactions of lung tissue (e.g. after repeated administration), which can eventually result into long-term adverse effects like fibrosis or neoplastic lesions. It has recently been demonstrated that AEII cells play a role in CeO<sub>2</sub> nanoparticle induced lung fibrosis [16]. Furthermore, it is known that AEII cells are a potential progenitor for lung tumors. As reviewed by Oberdörster [17] during particle-related inflammation, the recruited immune cells release growth factors and induce oxidative stress by the production of reactive oxygen species (ROS) for host defense. ROS can cause DNA damage, growth factors stimulate cell proliferation and by this the risk of tumor formation is increased. This hypothesis includes the well investigated process of secondary genotoxicity which is often accompanied by a present overload situation [18]. In contrast, little is known about primary mechanisms of genotoxicity, which are attributed to direct particle effects, like ROS generation due to surface reactivity [18]. Investigations of respective effects need to be done at absent inflammation. Less knowledge is published in how far CeO<sub>2</sub> nanoparticles react via the described molecular mechanisms and if they bear a carcinogenic potential after inhalation. Several *in vivo* inhalation studies demonstrate the induction of inflammatory reactions [19–26]. However, the majority of these studies most likely describe effects occurring during a present overload situation. Pro-oxidative but also anti-oxidative effects have been demonstrated for CeO<sub>2</sub> nanoparticles [19, 27–32]. Furthermore, some research indicates a genotoxic potential *in vivo* (intratracheal or oral application) [30, 33, 34] or *in vitro* [29, 35]. In contrast, first results from the chronic study mentioned earlier as well as the related dose-range finding study indicate no genotoxic effects for CeO<sub>2</sub> [22, 36]. Investigations of Ma et al. [16, 37, 38] indicate fibrosis induction after CeO<sub>2</sub> intratracheal instillation. More mechanistic information is needed for better understanding of partially contrary hypotheses. This includes the contribution of inflammation and overload on the one hand, and the particle's reactivity on the other hand, to the respective molecular events. Also, the use of very high nanoparticle concentrations in most available studies requires more research on lower dose levels.

Since the major share of the inhaled nanoparticle dose usually deposits in the respiratory organs and is eliminated via mechanisms of pulmonary clearance, extra-pulmonary translocation of a smaller particle fraction is a frequently detected concomitant effect. Aalapati et al. [19] measured Ce contents in different extra-pulmonary organs after 28-day exposure in mice, with highest levels

**Table 1 Summary of conventional endpoints**

Investigation	CeO <sub>2</sub>	BaSO <sub>4</sub>
Retention analytics	↑ lung burden (time- and concentration-dependent); ↓ clearance ( $\geq 1.0 \text{ mg/m}^3$ )	↑ lung burden (time-dependent); rapid clearance
Hematology/ clinical chemistry (d90 + 1rec)	↑ blood neutrophils	NAD
BAL analysis	↑ neutrophils, lymphocytes, total protein, LDH, $\beta$ -glucuronidase (time-/concentration-dependent); post-exposure persistency	↑ neutrophils; no post-exposure persistency
Histopathology	↑ particle-laden macrophages and inflammatory cell infiltrations (alveolar/interstitial/lymphoid tissue), bronchiolo-alveolar hyperplasia and fibrosis; post-exposure persistency	↑ particle-laden macrophages and inflammatory cell infiltrations; intra-epithelial eosinophilic globules and mucus cell hyperplasia in the nasal cavity; partly post-exposure persistency
Immunohistochemistry	↑ $\gamma$ -H2AX, 8-OHdG (genotoxicity); ↑ Ki-67 (proliferation); post-exposure persistency	↑ Ki-67 (proliferation); partly post-exposure persistency

NAD no abnormalities detected

in liver and kidney and particle-related histopathological changes of the respective organs. Other *in vivo* studies display comparable effects for CeO<sub>2</sub> nanoparticles [30, 39–43].

Potential mechanisms of action, especially regarding carcinogenicity of CeO<sub>2</sub> and BaSO<sub>4</sub> nanoparticles, were examined in this study. The highly sensitive method of gene expression analysis aims on the identification of early biomarkers for nanoparticle-related effects, especially those occurring after long-term exposure to realistic, low substance levels. The inclusion of low CeO<sub>2</sub> nanoparticle concentrations should create a situation of absent overload and inflammation to identify substance-related pro-oxidative, pro-proliferative or apoptotic as well as genotoxic effects. We focused on AEII cells as they are potential key players in (particle induced) pulmonary toxicity. The contribution of extra-pulmonary translocation to nanoparticle toxicity mechanisms motivated additional examinations of liver and kidney tissue as organs responsible for substance elimination. The identification of early biomarkers after acute to subchronic nanoparticle exposure creates a step towards the reduction of cost-intensive, animal-consuming long-term *in vivo* studies. Moreover, the *in vivo* markers should serve as basis for further investigations in an *in vitro* nanoparticle-exposure setup to intensify the focus on alternatives to animal testing.

## Results

### Conventional endpoints according to OECD TG 413

The obligatory investigations of the 90-day inhalation toxicity study according to OECD TG 413 were comprehensively reported elsewhere [1] and are briefly summarized in Table 1. We detected increasing lung burden levels for both nanomaterials with reduced clearance

halftimes of cerium at concentrations of  $\geq 1.0 \text{ mg/m}^3$ . Contrastingly, barium was rapidly cleared from the lung. The response of lung tissue and associated cell populations was dominated by inflammatory reactions. Particle-laden macrophages and inflammatory cell infiltrations, directed by neutrophils were detected in histopathology and bronchoalveolar lavage (BAL) analysis. Immunohistochemistry markers for genotoxicity (CeO<sub>2</sub> only) and cell proliferation were increased with ongoing exposure. Effects remained persistent up to 90 days subsequent to CeO<sub>2</sub>, and although to a much lower extent also after BaSO<sub>4</sub> exposure.

### Gene expression analysis in AEII cells

For AEII cells five different profiler PCR arrays (inflammatory cytokines and receptors, oxidative stress, DNA repair, apoptosis, lung cancer) were analyzed. In total, 34 genes were regulated and are listed in Table 2 and Additional file 1: Table S1. An overall upregulation of gene expression has been observed rather than downregulation. Switches between up- and downregulation of one specific gene has been detected rarely, therefore the direction of gene regulation could be determined quite explicit for most of the genes. Furthermore, the overlap between the regulated genes in response to both substances was quite high (> 60% similarity). The number of regulated genes increased with ongoing exposure time and increasing CeO<sub>2</sub> concentration (Fig. 1). Analysis of gene distribution over the different pathways revealed major contribution of inflammatory mediators at all time points (Fig. 2). All other pathways yielded up to four regulated genes. Inflammatory- and oxidative stress-related gene numbers increased in response to CeO<sub>2</sub>. Also in response to BaSO<sub>4</sub> a time-dependent increase of the number of regulated genes was detected. However, the

distribution over the five specified groups of mediators did not increase significantly. In total, 30 different genes were affected by CeO<sub>2</sub> and 25 genes by BaSO<sub>4</sub> exposure. The difference was mainly due to a lower number of inflammatory mediators regulated by BaSO<sub>4</sub>. Data for the most promising genes regarding their function as potential marker for nanoparticle-related effects and linked mechanisms of action are displayed individually in the following sections. Figure 15 shows an overview of assumed mechanistic relationships between the different cell types and effects involved in CeO<sub>2</sub> nanoparticle responses.

#### **Inflammatory cytokines and receptors**

The chemokines Ccl2, Ccl7, Ccl17 and Ccl22 (Fig. 3a–d) showed the most distinct upregulation of all inflammatory mediators tested. Regulation was highest after 90 days exposure to 3.0 mg/m<sup>3</sup> CeO<sub>2</sub>. Especially Ccl22 (Fig. 3d) showed a very high response to CeO<sub>2</sub> with a gene expression up to 19-fold higher than the control group. The regulation pattern for these four chemokines is quite similar. The inflammatory mediators Ccl3, Ccl4, Ccl24, Il-1α, Il-1β, Il-1rn were upregulated at low CeO<sub>2</sub> concentrations (0.1, 0.3 mg/m<sup>3</sup>) with a similar expression pattern (Fig. 3e–i). Although slight upregulation was detected for several mediators after 28 days, effects were highest after 90 days exposure. In contrast, BaSO<sub>4</sub> only affected Ccl2, Ccl7, and Ccl22.

#### **Oxidative stress**

Four genes related to oxidative stress were regulated after CeO<sub>2</sub> nanoparticle exposure (Table 2). The highest responses were detected for Lpo and Noxo1 with a concentration- and time-dependent increase (Fig. 4). Expression levels exceeded the fold regulation cut off already at 0.3 mg/m<sup>3</sup> CeO<sub>2</sub> nanoparticle exposure and reached values up to 56-fold higher compared to clean air inhalation after 90 days exposure to 3.0 mg/m<sup>3</sup> CeO<sub>2</sub>. Noxo1 was significantly upregulated after 28 and 90 days in response to the highest concentration of CeO<sub>2</sub>. BaSO<sub>4</sub> exposure revealed a total number of five regulated genes related to oxidative stress (Table 2). Lpo was affected in a similar way as after CeO<sub>2</sub> exposure, with a peak fold regulation of 25. Noxo1 was upregulated only after 28 days exposure to BaSO<sub>4</sub>.

#### **DNA repair and apoptosis**

Three genes related to DNA repair were regulated (Table 2), whereas Exo1 showed the most distinct regulation (data not shown). The impact of BaSO<sub>4</sub> on Exo1 expression was higher than effects of CeO<sub>2</sub>. Birc5, an apoptosis-related gene was slightly upregulated after 90-day nanoparticle exposure (data not shown).

#### **Lung cancer**

The lung cancer pathway revealed seven regulated genes (Table 2). The strongest response was detected for Mmp12 (Fig. 5). Fold regulation values markedly increased with ongoing CeO<sub>2</sub> nanoparticle exposure and increasing concentration. BaSO<sub>4</sub> effects were lower, but still caused significant upregulation of Mmp12 after 90 days.

#### **Analysis of protein expression in the alveolar compartment**

For the pathways inflammation, oxidative stress and lung cancer, the following regulated genes were investigated regarding their protein expression in either BAL or lung tissue of CeO<sub>2</sub> and BaSO<sub>4</sub> exposed animals: Ccl2, Ccl20, Il-1α and Il-1β (BAL analysis), Lpo and Mmp12 (immunohistochemistry of lung tissue).

#### **Ccl2 levels in bronchoalveolar lavage**

While Ccl20, IL-1α, and IL-1β protein levels in BAL did not change in response to nanoparticle exposure, Ccl2 was markedly increased with ongoing CeO<sub>2</sub> exposure and increasing concentration (Fig. 6). In addition to gene expression analysis, mediator levels in BAL were also measured during post-exposure of up to 90 days. Although a slight decrease of Ccl2 levels was observed in this phase, elevated protein expression was overall persistent. BaSO<sub>4</sub> also significantly affected Ccl2 protein expression in BAL.

#### **Immunohistochemical analysis of Lpo and Mmp12**

Since gene expression of Lpo and Mmp12 was highly upregulated in AEII cells, immunohistochemistry was used to evaluate the development of their protein level. Figures 7 and 8 exemplarily show tissue sections of the alveolar region of rats exposed to clean air, 3.0 mg/m<sup>3</sup> CeO<sub>2</sub>, or 50.0 mg/m<sup>3</sup> BaSO<sub>4</sub> for 90 days. The red colored signal indicates increased protein expression of Lpo (Fig. 7) or Mmp12 (Fig. 8) in response to both materials, while clean air did not cause any response. Lpo was detected in the alveolar epithelia in close proximity to the opening of the terminal bronchioli in regions of accumulated particle-laden macrophages and induced inflammation. The Lpo positive cells were morphologically consistent with AEII cells. Furthermore, no significant levels were measured in alveolar macrophages. This indicates that the increased Lpo gene expression in AEII cells caused also increased Lpo protein levels in the same cells. Lpo positive areas were additionally quantified per total tissue area. This analysis revealed an increasing signal with ongoing nanoparticle exposure, significant after 90 days for both substances (Fig. 9). The effect of CeO<sub>2</sub> was higher compared to BaSO<sub>4</sub> according to gene expression results. This is also visible in Fig. 7. The lung tissue

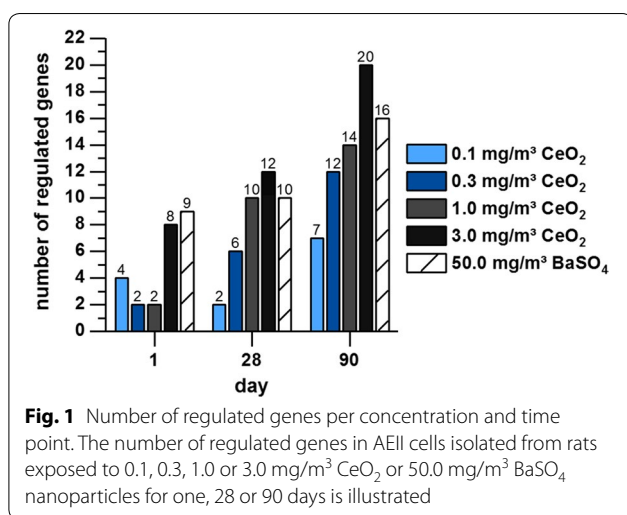
**Table 2 Gene regulation in AELI cells in response to CeO<sub>2</sub> and BaSO<sub>4</sub> after different exposure periods**

Array	Gene	CeO <sub>2</sub>			BaSO <sub>4</sub>			
		1 day	28 days	90 days	1 day	28 days	90 days	
Inflammatory cytokines and receptors	Ccl3	C–C motif chemokine ligand 3		↑	↑			
	Ccl17	C–C motif chemokine ligand 17		↑	↑			
	Cx3cr1	C–X3–C motif chemokine receptor 1	↑		↓			
	Il1a	Interleukin 1 alpha		↑	↑			
	Il1β	Interleukin 1 beta		↑	↑			
	Il1rn	Interleukin 1 receptor antagonist		↑	↑			
	Tnfsf4	Tumor necrosis factor superfamily member 4			↑↓			
	Ccl2	C–C motif chemokine ligand 2		↑	↑		↑	
	Ccl4	C–C motif chemokine ligand 4		↑	↑		↓	
	Ccl7	C–C motif chemokine ligand 7			↑		↑	
	Ccl11	C–C motif chemokine ligand 11	↑			↑		
	Ccl20	C–C motif chemokine ligand 20	↓	↑	↑↓	↓	↑	
	Ccl22	C–C motif chemokine ligand 22		↑	↑		↑	
	Ccl24	C–C motif chemokine ligand 24	↑	↑	↑		↑	
	Pf4	platelet factor 4			↑		↑	
	Cxcl9	C–X–C motif chemokine ligand 9	↓		↑		↑	
	Cd40lg	CD40 ligand	↓			↓		
	Il2rb	Interleukin 2 receptor, beta			↓	↓		
	Oxidative stress	Lpo	Lactoperoxidase		↑	↑	↑	↑
		Noxo1	NADPH oxidase organizer 1		↑	↑		↑
Hba1		Hemoglobin alpha, adult chain 2	↓	↓	↓	↓	↓	
Scd1		Stearoyl-Coenzyme A desaturase 1		↑	↓		↓	
Krt1		Keratin 1				↑	↑	
DNA repair	Msh5	mutS homolog 5	↑					
	Exo1	Exonuclease 1	↓		↑	↓	↑	
	Mutyh	MutY homolog ( <i>E. coli</i> )	↓				↑	
Apoptosis	Birc5	Baculoviral IAP repeat-containing 5			↑	↑	↑	
Lung cancer	Cyp1b1	Cytochrome P450, family 1, subfamily b, polypeptide 1		↑↓				
	Fabp4	Fatty acid binding protein 4		↑	↑		↓	
	Mmp12	Matrix metalloproteinase 12		↑	↑		↑	
	Opcml	Opioid binding protein/cell adhesion molecule-like	↑	↑		↑	↑	

**Table 2 continued**

Array	Gene	CeO <sub>2</sub>			BaSO <sub>4</sub>		
		1 day	28 days	90 days	1 day	28 days	90 days
	Tcf21						↓
	Thbs2						↑
	Top2a					↑	
Total	34	11	18	24	9	10	15

↑ upregulation; ↓ downregulation; ↑↓ up- or downregulation (differences between CeO<sub>2</sub> dose groups); cut-off: FR ≤ -2.0 or ≥ 2.0



overview sections contain more areas of CeO<sub>2</sub> particle-laden macrophages with positive Lpo signal in epithelial cells (Fig. 7C) than BaSO<sub>4</sub> related signals (Fig. 7E). As seen in Fig. 7D, the brown colored CeO<sub>2</sub> particles accumulated in macrophages are histologically visible. The analyzed tissue was therefore further used for quantification of cerium (Fig. 10). The signal was significantly exceeding control levels and was increasing with ongoing particle exposure.

Mmp12 protein levels were increased after 28 and 90 days nanoparticle exposure, but did not yield any significance, due to high variation between individual tissue slides (Fig. 9b). The picture of the lung sections (Fig. 8) indicates that the positive signal originates predominantly from alveolar macrophages rather than epithelial cells. However, single Mmp12 positive AEII cells were also detectable.

#### Gene expression analysis of liver and kidney tissue

In liver and kidney tissue 14 and 18 genes respectively were regulated in total (Table 3, Additional file 1: Table S1). Similar to the AEII cells a high response concerning

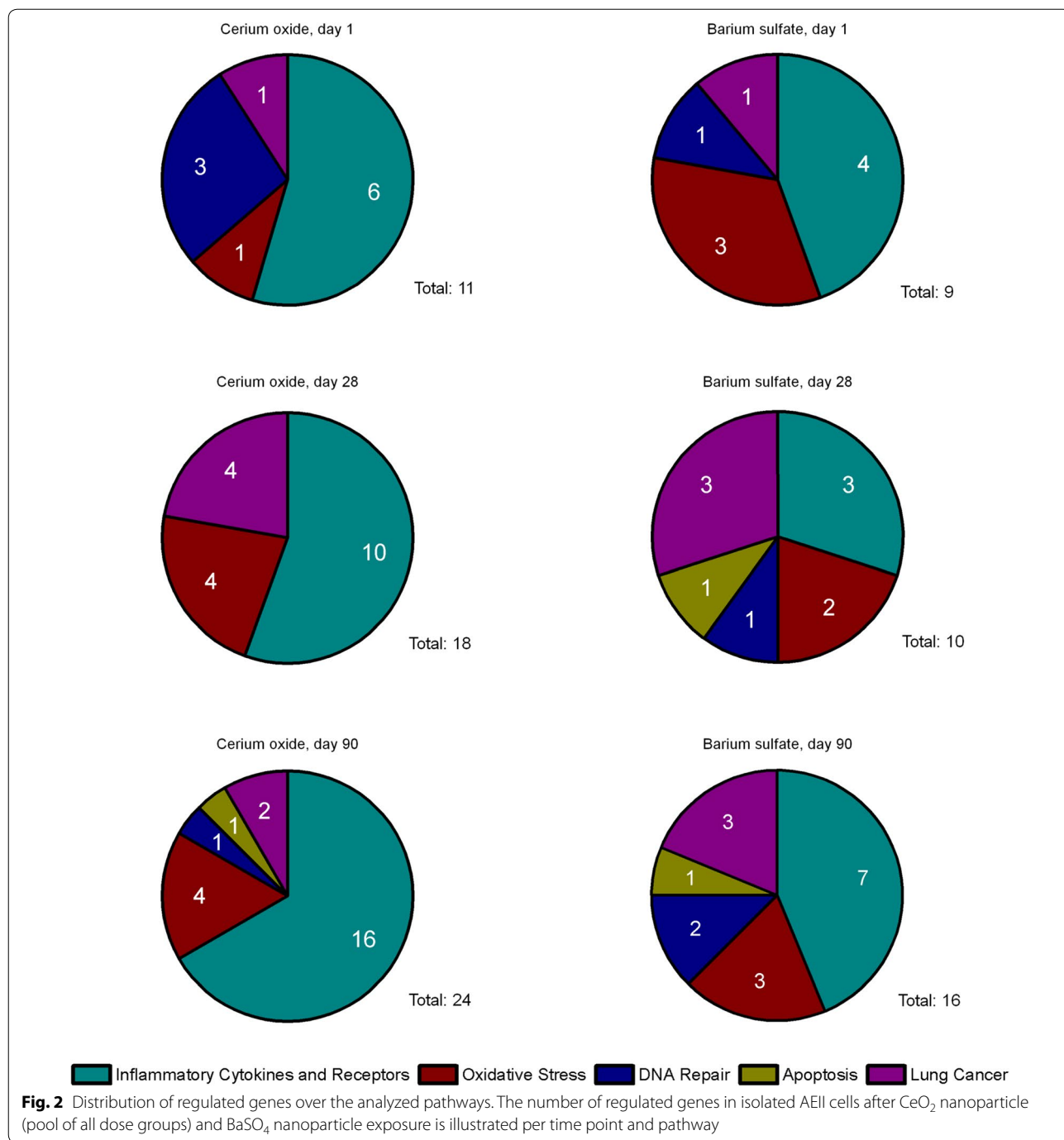
the amount of regulated genes was seen for the endpoint inflammation (50% of total for liver, ~ 30% of total for kidney; Fig. 11). However, in kidney tissue even more genes were found to be related to oxidative stress, most of them downregulated. In both tissues a minor portion of the regulated genes was DNA repair-related. Comparison of both substances indicated a higher response of gene regulation to CeO<sub>2</sub> than to BaSO<sub>4</sub>.

#### Nanoparticle retention in liver and kidney tissue

Since some changes in gene expression were detected in liver and kidney tissue after nanoparticle exposure, we determined the amount of Ce in both organs. Figure 12 exemplarily shows the level of ionic, particulate and total Ce in the liver during and after 90 day exposure to 3.0 mg/m<sup>3</sup> CeO<sub>2</sub>. The overall amount is low, but there is a significant increase in Ce levels with ongoing exposure and values decrease after the last day of exposure. Differences in the level of ionic and particulate Ce are marginal. A switch from more ionic to more particulate Ce with ongoing nanoparticle exposure and back to higher ionic levels during post-exposure was detected. Table 4 contains all Ce levels measured in liver and kidney for the mid and high dose group. 1.0 mg/m<sup>3</sup> CeO<sub>2</sub> caused slightly lower values and a similar trend as seen in the high dose group, with peak levels of 2 µg/liver after 90 days exposure. The lower Ce dose groups and BaSO<sub>4</sub> were not measured at this point.

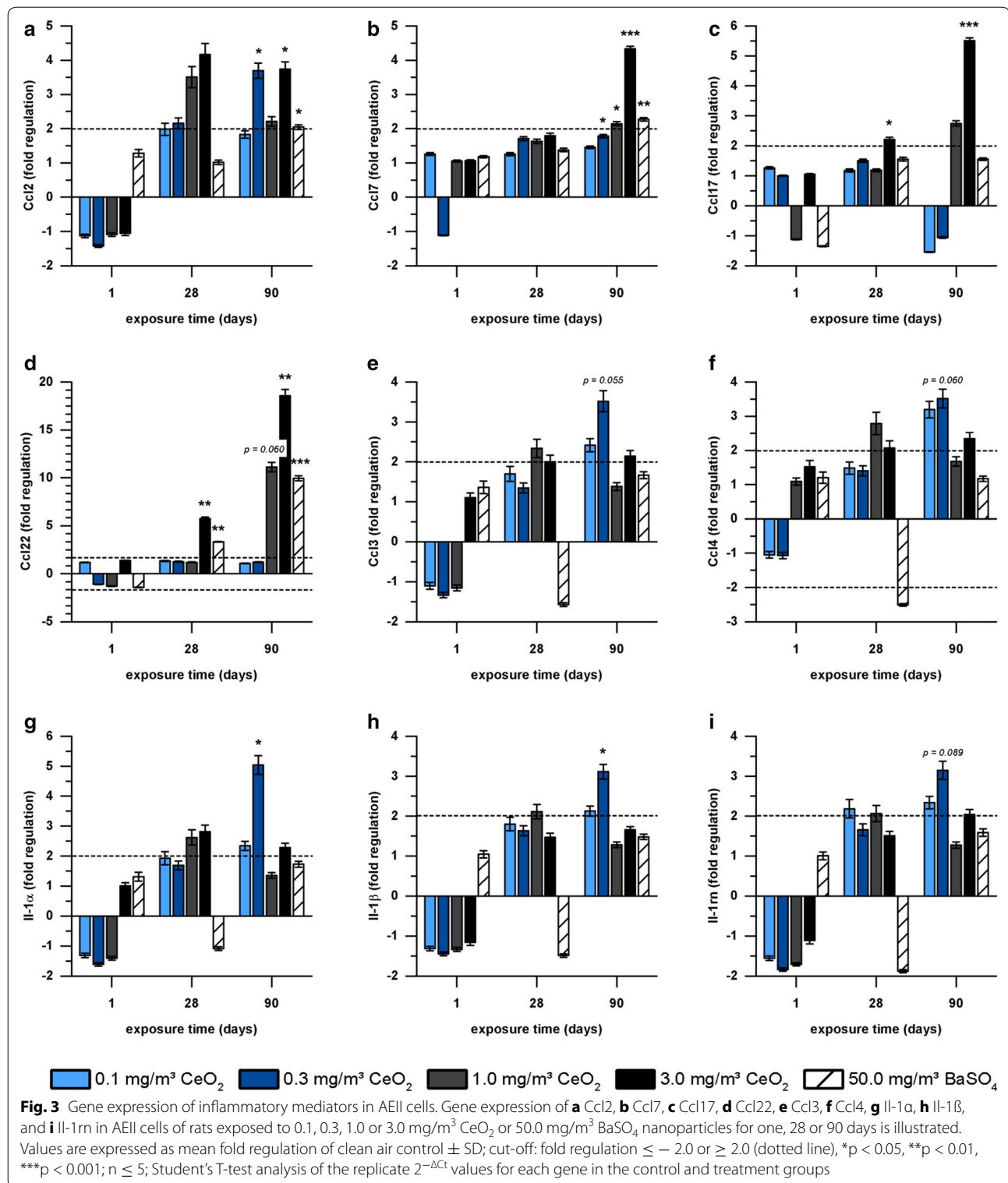
#### Discussion

Gene expression analysis is a highly sensitive method, which can yield valuable supportive information on a mechanistic level. Therefore, the gene expression analysis described here was performed as extension of a 90-day inhalation toxicity study on nanomaterial according to OECD TG 413. It aimed on the identification of early biomarkers predicting effects of subacute to chronic nanoparticle exposure. Results of the guideline required parts of the study are discussed in detail elsewhere [1]. Briefly, a marked pulmonary inflammation was detected



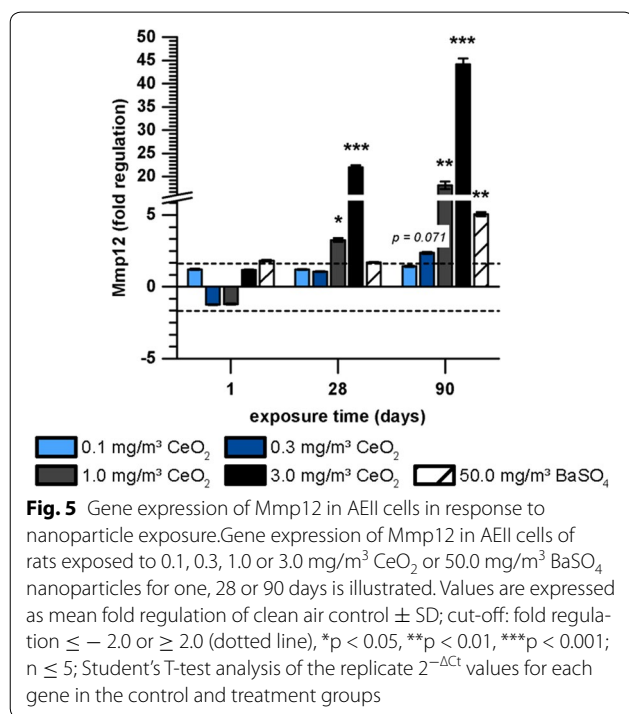
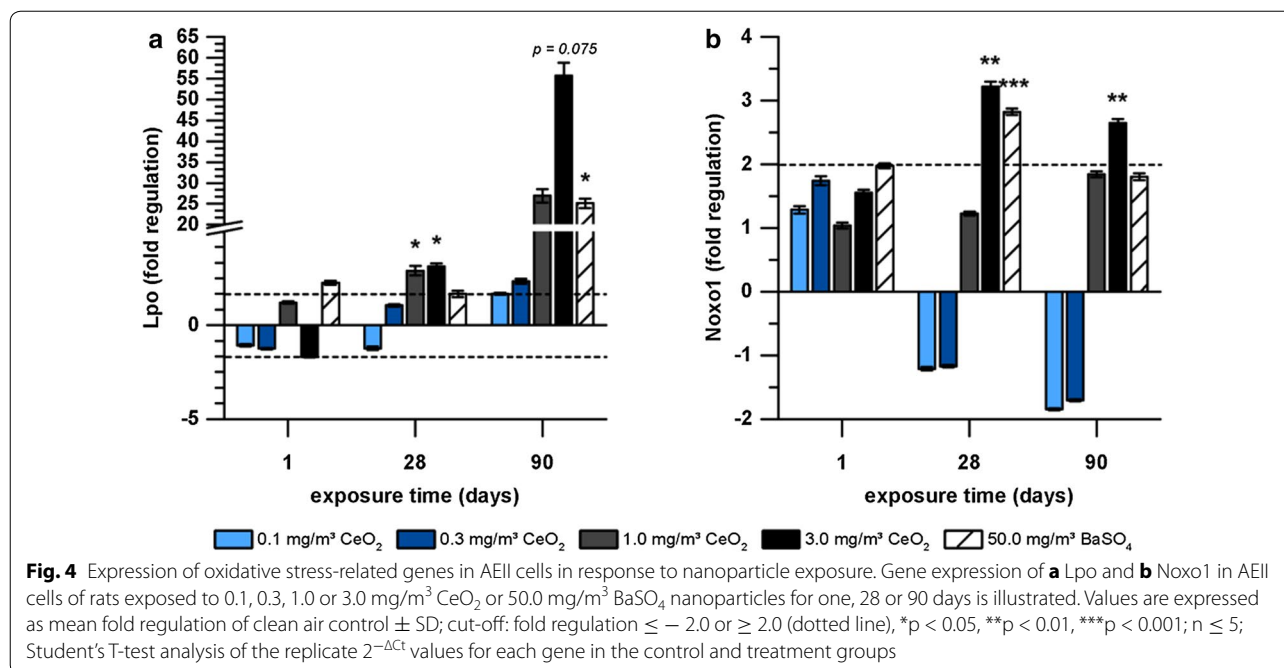
in response to 3.0 mg/m<sup>3</sup> CeO<sub>2</sub> nanoparticle inhalation, showing increasing severity with ongoing particle exposure and post-exposure persistency. This particle concentration most likely provoked lung overload, indicating that the inflammation was caused by oversaturated macrophages and related impaired lung clearance. Histopathological findings suggest the risk of long-term effects like fibrosis, resulting from the chronic inflammation

reaction. For the mid concentration (1.0 mg/m<sup>3</sup> CeO<sub>2</sub>) also signs of inflammation accompanied by slightly impaired lung clearance were detected. Depending on the calculation method, overload is assumed to be present or absent and therefore making a clear conclusion difficult. At lower CeO<sub>2</sub> concentrations (0.1 and 0.3 mg/m<sup>3</sup>) no signs of inflammation and overload were detected. BaSO<sub>4</sub> nanoparticles (50.0 mg/m<sup>3</sup>) also caused



mild inflammatory cell infiltrations in the alveolar space, although major effects were restricted to the nasal cavity, due to particle accumulation. Interestingly, despite the

high concentration administered to the animals, BaSO<sub>4</sub> was cleared rapidly from the lung without provoking overload.



#### Local alveolar effects of CeO<sub>2</sub> nanoparticles

An overview of CeO<sub>2</sub> nanoparticles' influence on the alveolar compartment in terms of inflammation, oxidative stress and tissue degradation is depicted in Fig. 15.

The described inflammation was reflected by gene expression analysis. In AEII cells a total number of 34

genes were regulated after nanoparticle exposure and thereof 18 were chemokines or interleukins, responsible for immune cell activation and recruitment. This matches inflammatory cell infiltrations in lung tissue and increasing neutrophil and lymphocyte levels in BAL detected in the main study [1]. A major part of the effects exacerbate time- and concentration-dependent, which was reflected by two different phenomena on mRNA level: (1) increase in total number of regulated genes, (2) increase in fold regulation of the individual genes.

Pulmonary immune responses imply the complex interaction between different inflammatory cell types, but also respiratory epithelial cells. In particular AEII cells are suggested to release inflammatory mediators. Most distinct regulation in these cells was detected for the C-C motif chemokines Ccl2, Ccl7, Ccl17 and Ccl22 after 1.0 and 3.0 mg/m<sup>3</sup> CeO<sub>2</sub> nanoparticle exposure. Ccl2 and Ccl7 are closely related chemoattractant proteins, which bind to the same receptor (Ccr2) and cause similar responses, like macrophage, lymphocyte and neutrophil recruitment [44]. Ccl17 and Ccl22 also react via a common receptor (Ccr4). They are involved in activation of CD4<sup>+</sup> T-lymphocytes and monocytes [45, 46]. Our results show upregulation of all these chemokines in response to CeO<sub>2</sub> nanoparticle exposure and correlations between the related mediators Ccl2/Ccl7 and Ccl17/Ccl22 (Fig. 13a, b). At exposure conditions resulting in high gene regulation (90 days exposure, CeO<sub>2</sub> concentration  $\geq 1.0$  mg/m<sup>3</sup>) also significant changes in the amount of target cells for those mediators have been detected in

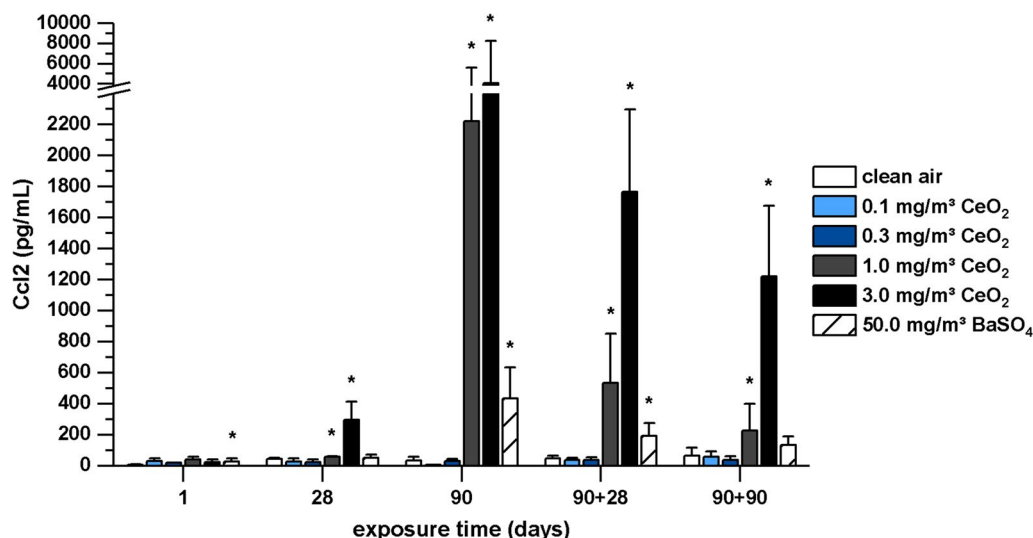


**Fig. 6** Ccl2 levels measured in bronchoalveolar lavage. Rats were exposed to clean air, 0.1, 0.3, 1.0, and 3.0 mg/m<sup>3</sup> CeO<sub>2</sub> nanoparticles or 50.0 mg/m<sup>3</sup> BaSO<sub>4</sub> nanoparticles. Ccl2 levels were determined after one, 28 and 90 days exposure and 28 and 90 days after the end of 90 days exposure (90 + 28, 90 + 90). Values are expressed as mean + SD, \*p ≤ 0.05 vs. clean air control, n ≤ 5; Kruskal–Wallis–ANOVA with Mann–Whitney U-test as post hoc analysis

histopathology and/or BAL (particle-laden macrophage accumulations, increased lymphocyte levels) [1]. Until now less was known regarding the expression of the mentioned chemokines in AEII cells in general or in response to nanoparticles. Several studies indicate Ccl2 production in isolated AEII cells after different stimuli [3, 47–52]. Cxcl2 or Ccl2 mRNA expression in either isolated AEII cells or alveolar epithelial cell lines has been described already in response to quartz exposure [6, 53, 54] and Chen et al. [8] demonstrated the expression and release of different Cxcl-motif chemokines by AEII cells after intra-tracheal instillation of carbon nanoparticles and assumed AEII cells to be the major key player in this neutrophil-driven response.

Lower, non-overload concentration levels should help to evaluate potential substance related effects. Our previous investigations indicated that at a concentration of 1.0 and even 3.0 mg/m<sup>3</sup> CeO<sub>2</sub> effects are likely not exclusively overload-related but also dependent on material-specific characteristics, because they did not induce a volumetric or specific surface-related lung overload [1]. The upregulation of chemokines is therefore to some extent substance related either. CeO<sub>2</sub> nanoparticle exposure at 0.1 and 0.3 mg/m<sup>3</sup> revealed gene regulation of inflammatory mediators, not markedly affected at higher dose levels (Ccl3, Ccl4, Il-1α, Il-1β, Il-1rn). Ccl3 and Ccl4 are two related mediators with the shared receptor Ccr5. They function as chemoattractant for mainly monocytes and lymphocytes and are expressed by a variety of cells, including inflammatory and epithelial cells [55]. Il-1α

and Il-1β both bind to the interleukin receptor and trigger chemokine release from target cells and immune cell activation. The antagonist Il-1rn competes with Il-1α and Il-1β for interleukin receptor binding and by this balances induced immune reactions. Evidence is given that Il-1α and Il-1β stimulate Ccl2 expression in AEII cells [3, 4, 51, 56]. Brabcová et al. [57] demonstrated in addition to Ccl2 effects on Ccl3, Ccl4, and Ccl17 levels in A549 cell cultures in response to Il-1β and graded this interleukin as a quite potent chemokine stimulant. Il-1β synthesis has also been found in stem cell-derived lung epithelial cells [58] and isolated mouse AEII cells exposed to TiO<sub>2</sub> nanoparticles [59]. So far, data on the influence of nano-CeO<sub>2</sub> on the release of the discussed mediators by AEII cells has not been reported by others. Only some measurements of Il-1β have been performed in BAL [19, 26] or lung tissue [30] of rodents treated with CeO<sub>2</sub>. However, since no cell type specific analysis was performed the cellular source of Il-1β remains unknown.

90 days exposure to concentrations of up to 0.3 mg/m<sup>3</sup> revealed significant upregulation of the respective mediators followed by a decrease to baseline levels in higher dose groups and highly correlated expression patterns between all mediators (Fig. 13c–l). Since the chemokines and interleukins indicate inflammation which was for this concentration not yet measurable in BAL analysis but clearly present at higher dose levels (BAL and histopathology) [1], the respective mediators might function as promising sensitive biomarkers for nanoparticle exposure on a gene expression level. Also, this gene

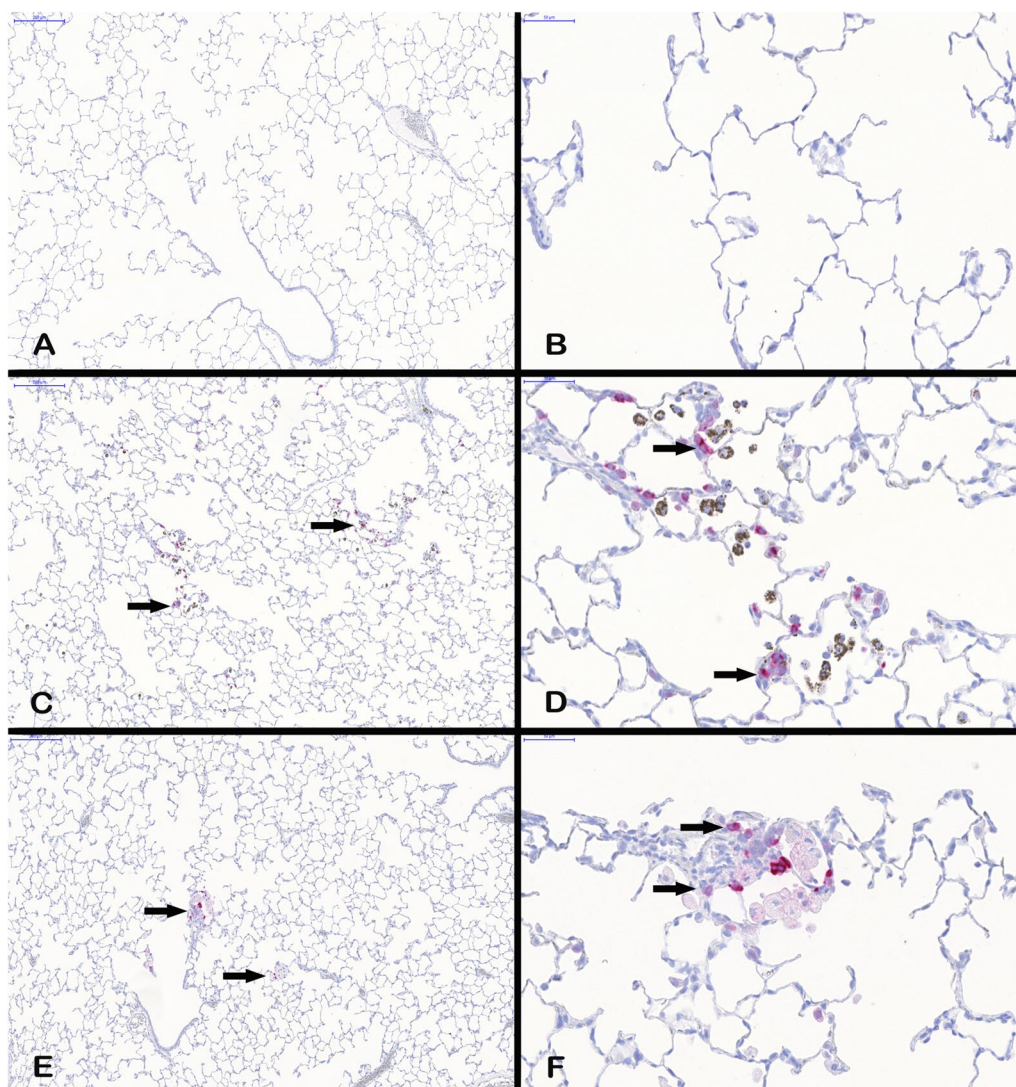


**Fig. 7** Lpo protein expression in lung tissue. All examples illustrate findings after 90-day nanoparticle exposure. **A** lung tissue overview,  $\times 10$ , and **B** detailed view,  $\times 40$ , after clean air exposure, **C** Lpo positive cells (arrows) in lung tissue overview,  $\times 10$ , and **D** detailed view,  $\times 40$ , after  $3.0 \text{ mg/m}^3 \text{ CeO}_2$  exposure, and **E** Lpo positive cells (arrows) in lung tissue overview,  $\times 10$ , and **F** detailed view,  $\times 40$ , after  $50.0 \text{ mg/m}^3 \text{ BaSO}_4$  exposure. The images show Lpo-positive cells counterstained with hematoxylin

regulation might indicate an early risk of induced pulmonary inflammation during long-term low dose exposure to  $\text{CeO}_2$  nanoparticles. In parallel to our 90-day study respective investigations will be provided by a long-term setup with the same  $\text{CeO}_2$  nanomaterial and concentrations as part of the European program on the regulatory testing of manufactured nanomaterials (NANoREG), in which potential toxic and carcinogenic effects during and after exposure periods of up to 1 year were investigated [BASE, Ludwigshafen, Germany, “combined chronic inhalation toxicity and carcinogenicity study with  $\text{CeO}_2$  and  $\text{BaSO}_4$ ”, (81|0661/10|170)]. The combination of both

studies constitutes the ideal base to prove and classify the meanings of the potential early signs for inflammatory effects discussed here.

It could be assumed that AEII cells support the defense against nanoparticles in second instance since upregulation of inflammatory mediators started at later stages of exposure and was dominated by chemokines stimulating monocytes and cells of the adaptive immune system (e.g. lymphocytes). Constant monocyte recruitment supports elimination of the rising particle amount and handling of overload conditions, lymphocytes are usually recruited for delayed defenses. Our histopathology and

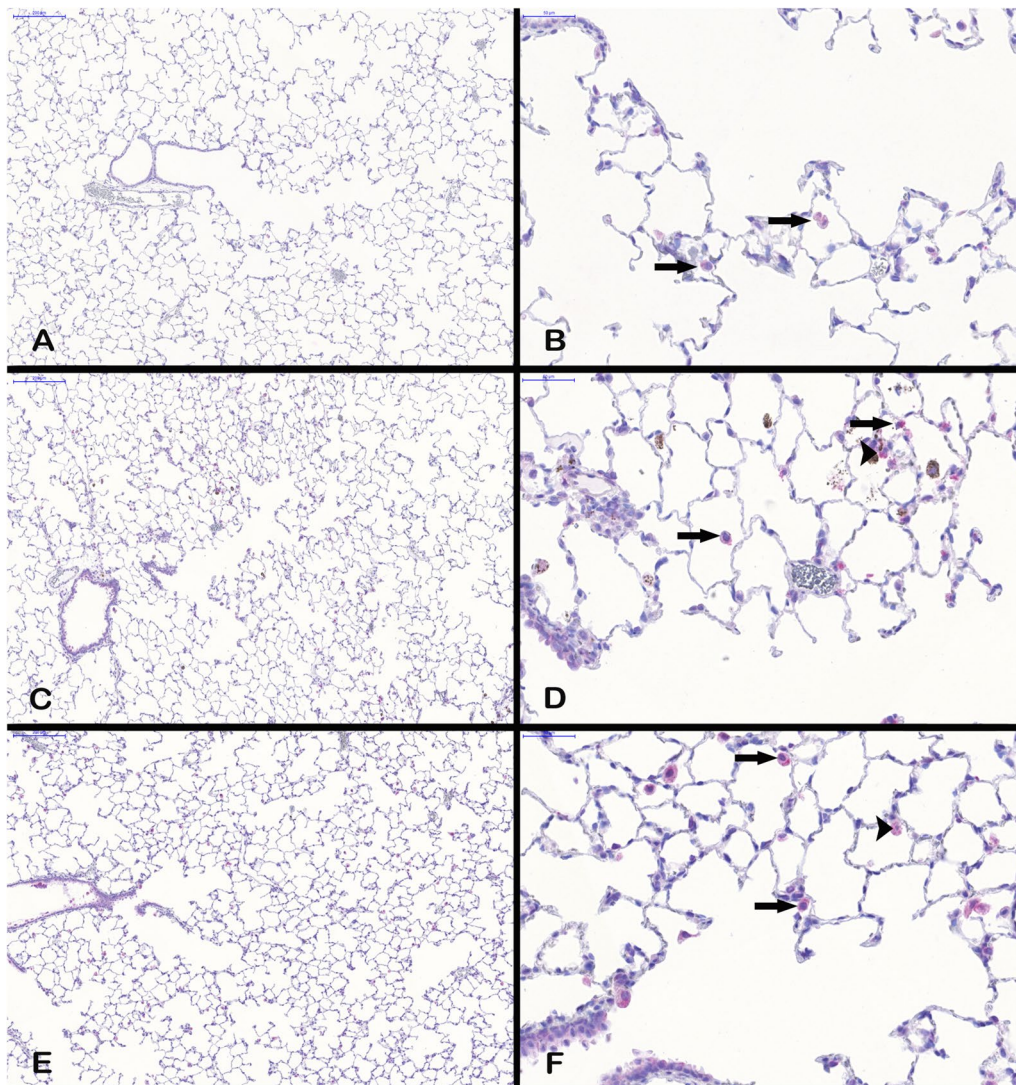
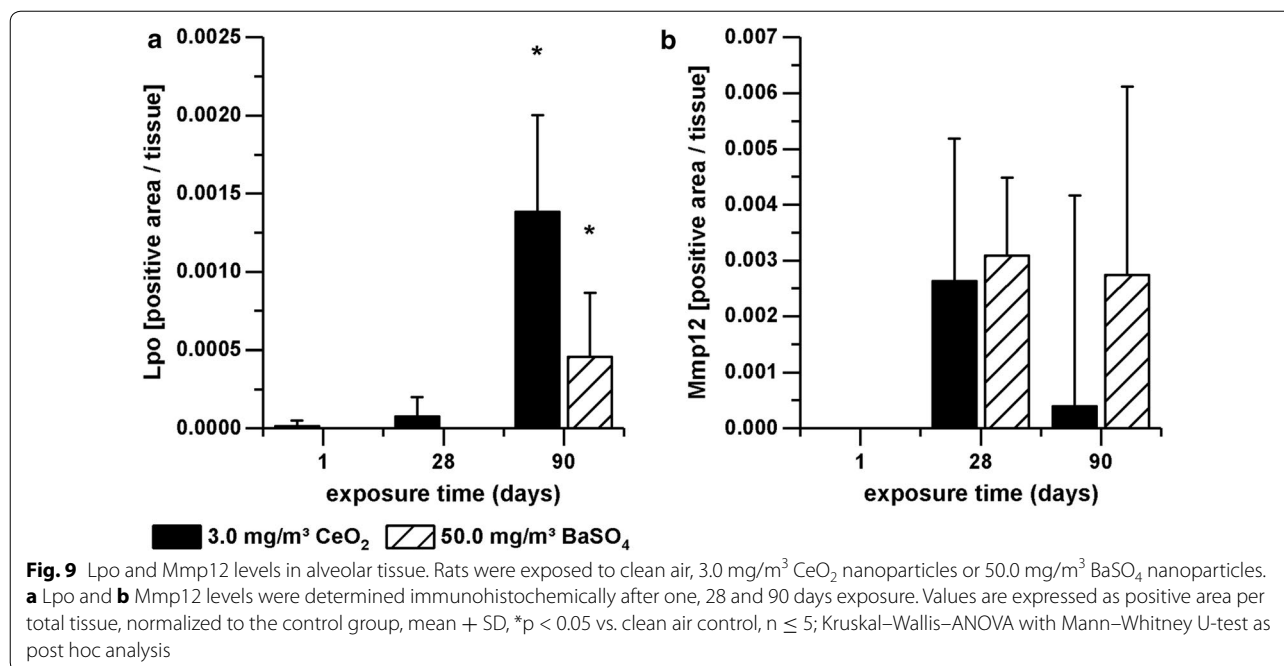


**Fig. 8** Mmp12 protein expression in lung tissue. All examples illustrate findings after 90-day nanoparticle exposure. **A** Mmp12 positive macrophages (arrows) in lung tissue overview ( $\times 10$ ) and **B** detailed view ( $\times 40$ ) after clean air exposure, **C** Mmp12 positive macrophages (arrows) and AELI cells (arrowhead) in lung tissue overview ( $\times 10$ ) and **D** detailed view ( $\times 40$ ) after  $3.0 \text{ mg/m}^3 \text{ CeO}_2$  exposure, and **E** Mmp12 positive macrophages (arrows) and AELI cells (arrowhead) in lung tissue overview ( $\times 10$ ) and **F** detailed view ( $\times 40$ ) after  $50.0 \text{ mg/m}^3 \text{ BaSO}_4$  exposure. The images show Mmp12-positive cells counterstained with hematoxylin

BAL analysis match this theory as we found neutrophilic inflammation at early stages of exposure, followed by increasing levels of lymphocytes [1]. Respective observations were accompanied by sustained presence of particle-laden macrophages.

Although inflammatory effects of  $\text{CeO}_2$  nanoparticle exposure were dominating signs of induced oxidative stress have additionally been detected. A marked time-dependent upregulation of Lpo mRNA and protein was measured in AELI cells. Protein analysis further identified the increased Lpo levels as being related to areas of particle-laden macrophage accumulations and inflammatory

cell infiltrations. Lpo catalyzes the conversion of thiocyanate to antibacterial hypothiocyanite by use of hydrogen peroxide and belongs to the non-immunological airway defense system. The respiratory Lpo defense system highly depends on  $\text{H}_2\text{O}_2$  and is influenced by the presence of inflammatory mediators [60]. Based on research with oxidized SWCNT evidence is given that Lpo functions in nanomaterial degradation [61]. Since  $\text{CeO}_2$  particles bear redox activity, an interaction with the Lpo defense system seems reasonable and supports substance related effects. The particles might be able to process  $\text{H}_2\text{O}_2$  by  $\text{Ce}^{3+}/\text{Ce}^{4+}$  redox cycling. Although respective



properties were reviewed from an anti-oxidative perspective, in terms of mimicking superoxide dismutase (SOD) or catalase activities, CeO<sub>2</sub> obviously has the potential to affect H<sub>2</sub>O<sub>2</sub> balance. The SOD like reaction includes the generation of H<sub>2</sub>O<sub>2</sub> from superoxide anion. This would favor the increase of extracellular H<sub>2</sub>O<sub>2</sub> and might cause elevated Lpo levels. Also other theories of oxidative stress generation, including lipid peroxidation [19] by the particles are conceivable. The catalytic activity thus claims consideration of both, pro- and anti-oxidative capacities.

Furthermore, an inflammation-related hypothesis for elevated Lpo levels could be based on respiratory burst. Inflammatory cells eliminate internalized material by the production of ROS. Neutrophils for instance release O<sub>2</sub><sup>-</sup> and H<sub>2</sub>O<sub>2</sub> in response to various stimuli [62]. Lung epithelial cells are further known to physiologically produce H<sub>2</sub>O<sub>2</sub> [63]. Bronchial epithelial cells have been shown to increase H<sub>2</sub>O<sub>2</sub> release in response to the inflammatory mediator IFN $\gamma$ , leading to stimulation of the Lpo defense system [60]. Such conditions might thus be responsible for imbalance of the system during inflammation (1.0 or 3.0 mg/m<sup>3</sup> CeO<sub>2</sub>), manifested by increased Lpo levels in AEII cells at hotspots of inflammation and the correlation between the amount of neutrophils in BAL and Lpo gene expression levels (Fig. 14a).

Another upregulated factor participating in ROS generation is Nox1, which is part of the transmembrane Nox enzyme complex and contributes to extracellular ROS production by intracellular consumption of NADPH [64]. It was significantly upregulated in response to 3.0 mg/m<sup>3</sup> CeO<sub>2</sub> when also a marked Lpo expression was observed. Van Klaveren et al. [65] demonstrated activation of a membrane bound NADPH oxidase-like system in isolated rat AEII cells and enzymatic generation of O<sub>2</sub><sup>-</sup> and H<sub>2</sub>O<sub>2</sub> in response to different stimuli. The potential contribution of this system to H<sub>2</sub>O<sub>2</sub> levels suggests a functional relationship between Nox1 and Lpo levels after CeO<sub>2</sub> nanoparticle exposure.

No clear evidence was given for effects on genotoxicity and apoptosis in AEII cells after CeO<sub>2</sub> nanoparticle

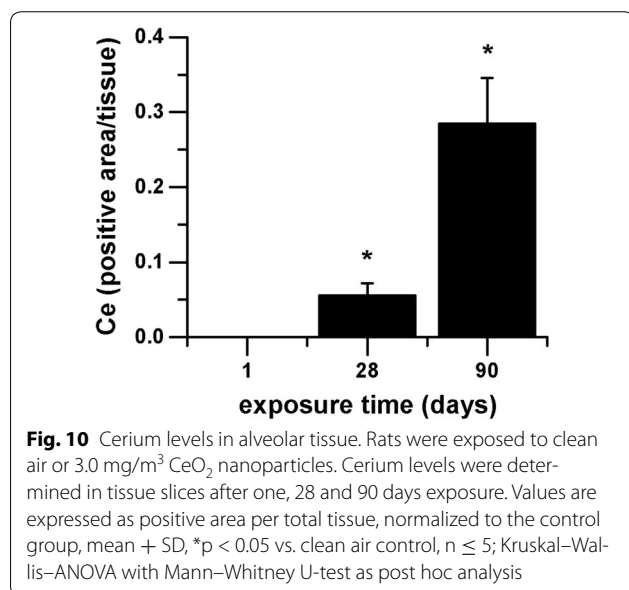


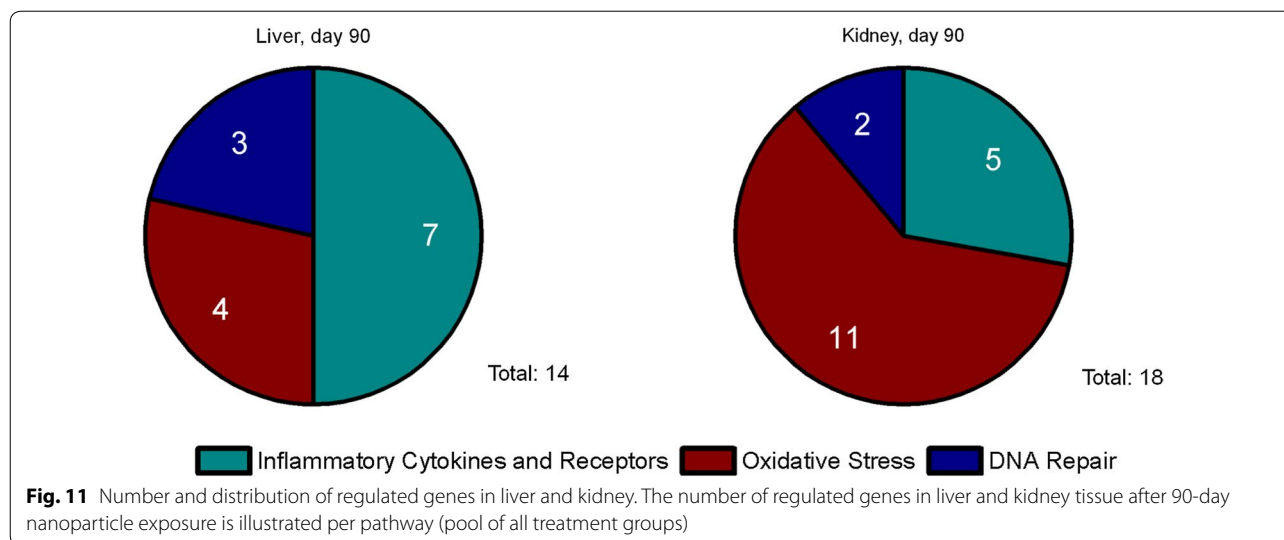
**Table 3 Gene regulation in liver and kidney in response to 90 days CeO<sub>2</sub> and BaSO<sub>4</sub> exposure**

Array	Gene	CeO <sub>2</sub>		BaSO <sub>4</sub>			
		Liver	Kidney	Liver	Kidney		
Inflammatory cytokines and receptors	Ccr2	Chemokine (C–C motif) receptor 2	↑		↑		
	Cx3cl1	Chemokine (C–X3–C motif) ligand 1	↑				
	Cxcl12	Chemokine (C–X–C motif) ligand 12	↓				
	Cxcr2	Chemokine (C–X–C motif) receptor 2	↑				
	Cxcr3	Chemokine (C–X–C motif) receptor 3	↑		↑		
	Il2rg	Interleukin 2 receptor, gamma	↑				
	Osm	Oncostatin M	↑	↓			
	Ccl2	Chemokine (C–C motif) ligand 2				↑	
	Ccl9	Chemokine (C–C motif) ligand 9		↑		↑	
	Cxcr5	Chemokine (C–X–C motif) receptor 5		↓			
	Spp1	Secreted phosphoprotein 1		↓			
	Oxidative stress	Gpx2	Glutathione peroxidase 2	↓	↓		
		Lpo	Lactoperoxidase	↑		↑	
Ncf2		Neutrophil cytosolic factor 2	↑	↓			
Scd1		Stearoyl-Coenzyme A desaturase 1	↑	↑	↑	↑	
Alb		Albumin		↑↓		↑	
Epx		Eosinophil peroxidase		↓			
Gclc		Glutamate-cysteine ligase, catalytic SU		↓			
Gclm		Glutamate cysteine ligase, modifier SU		↓			
Hba1		Hemoglobin alpha, adult chain 2		↓			
Mpo		Myeloperoxidase		↑			
Ngb		Neuroglobin		↓		↓	
Txnip		Thioredoxin interacting protein		↓		↓	
DNA repair		Lig4	Ligase IV, DNA, ATP-dependent	↑	↓	↑	
	Smug1	Single-strand-selective monofunctional uracil-DNA glycosylase 1	↑				
	Xrcc2	X-ray repair complementing defective repair in Chinese hamster cells 2			↑		
	Brca1	Breast cancer 1		↓			
Total	27		13	17	6	6	

↑ upregulation; ↓ downregulation; ↑↓ up- or downregulation (differences between dose groups); cut-off: FR ≤ - 2.0 or ≥ 2.0

exposure since no distinct gene regulation was measured for the tested DNA repair- or apoptosis-related genes.

However, we further found some indications for chronic particle related effects, including fibrosis and lung cancer. Mmp12 plays an important role in lung



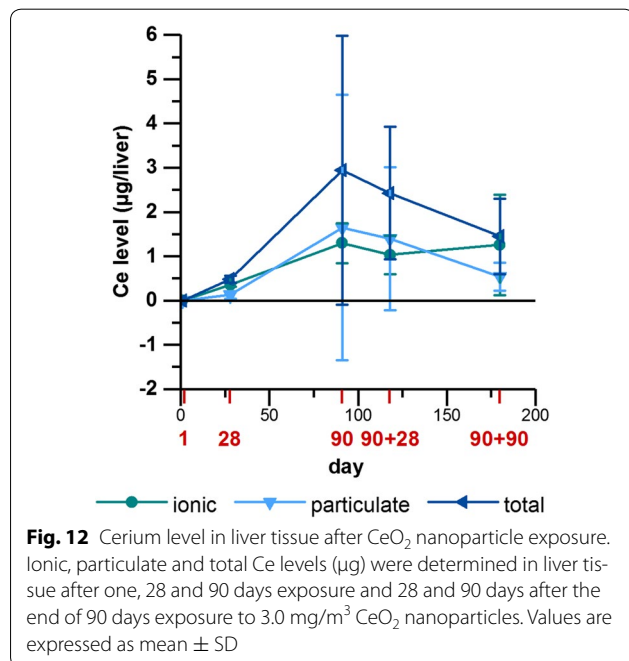
tissue remodeling and serves as marker for related acute and chronic lung diseases like fibrosis and COPD [66, 67]. Activated alveolar macrophages produce Mmp12 for neutrophil activation and release of neutrophil elastase. This leads to tissue degradation and finally emphysema development. The persistent neutrophil infiltrations measured during our previous investigations [1], accompanied by increased Mmp12 mRNA in lung epithelia indicate such mechanisms and the risk of developing chronic pathological changes during long-term exposure. Although immunohistochemical staining of lung tissue for Mmp12 did not reveal significantly elevated

protein levels, Mmp12 might serve as a valid marker for substance related mechanisms of action as mRNA upregulation occurs at absent lung overload with CeO<sub>2</sub> nanoparticles. Overexpression of Mmp12 has been described in mouse lungs after application of asbestos or TiO<sub>2</sub> nanoparticles [68, 69]. The latter caused parallel upregulation of Ccl2, 3, 4 and 7, which were also affected in our studies. Ma et al. [16] demonstrated the influence of CeO<sub>2</sub> nanoparticles on the development of fibrosis by induction of epithelial–mesenchymal transition of AEII cells after intra-tracheal instillation. Interestingly, disturbance of the Lpo defense system was demonstrated in relation to the pathology of cystic fibrosis [70]. The high correlation of both mediators (Fig. 14b) therefore might function as marker for fibrosis induction in AEII cells triggered through the early inflammation events. This hypothesis is further supported by very slight interstitial fibrosis measured in the main study (90 days post-exposure, 3.0 mg/m<sup>3</sup> CeO<sub>2</sub>) [1].

Figure 15 summarizes the potential relationship between the analyzed mediators and different cell types in response to nanoparticle exposure. Increased gene expression in AEII cells is assumed to affect inflammatory cells and the lung's oxidative balance. This might further lead to tissue degradation and long-term effects like fibrosis. Lpo, Mmp12 and the inflammatory mediators Ccl2, 7, 17, 22, 3, 4, Il-1 $\alpha$ , Il-1 $\beta$  and Il-1rn are promising marker genes for the mentioned effects.

#### Local alveolar effects of BaSO<sub>4</sub> nanoparticles

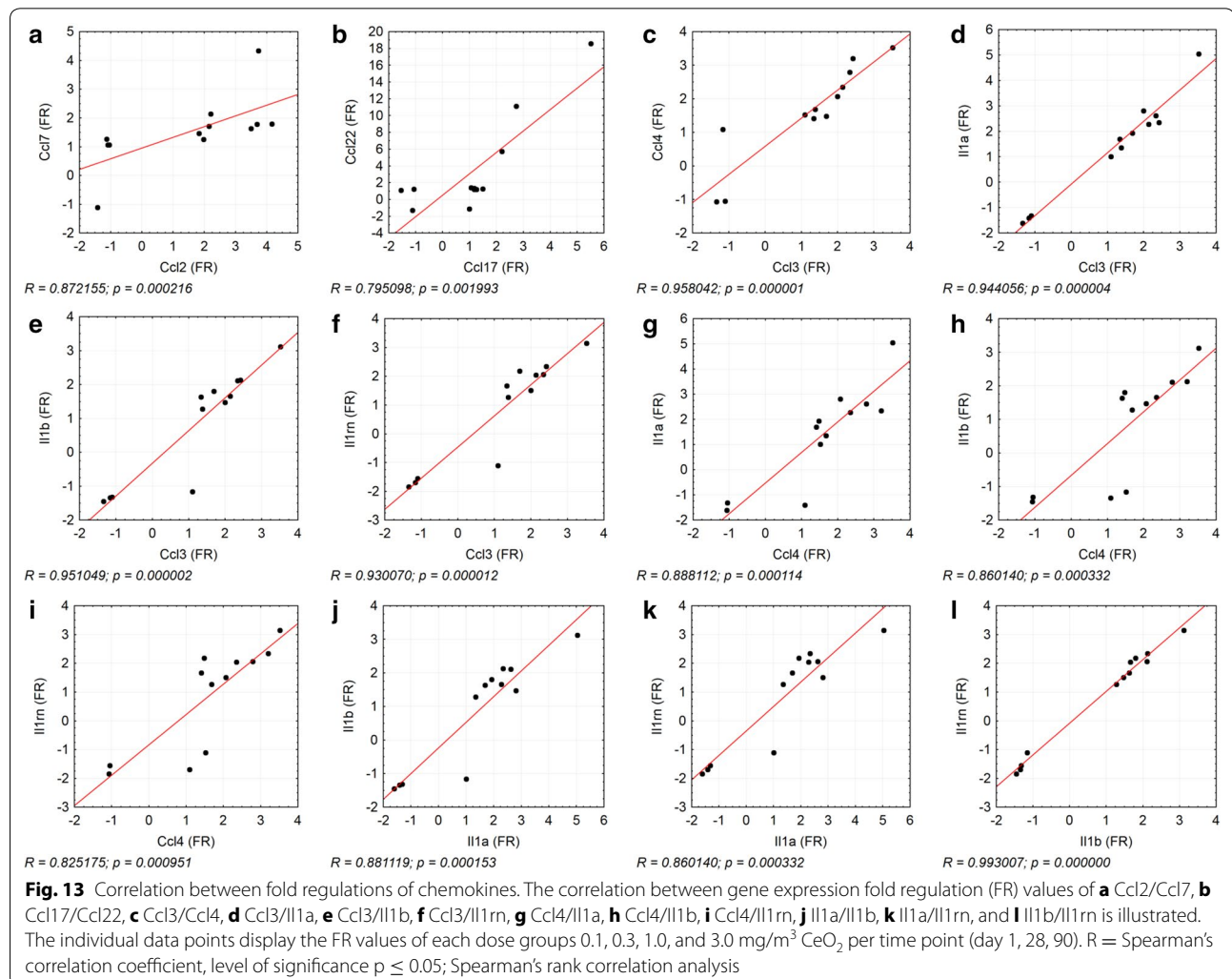
Considering BaSO<sub>4</sub> classification as chemically inert and non-toxic, a generally low and non-adverse response was expected. Therefore BaSO<sub>4</sub> NM-220 was selected as reference material without any specific toxicity in

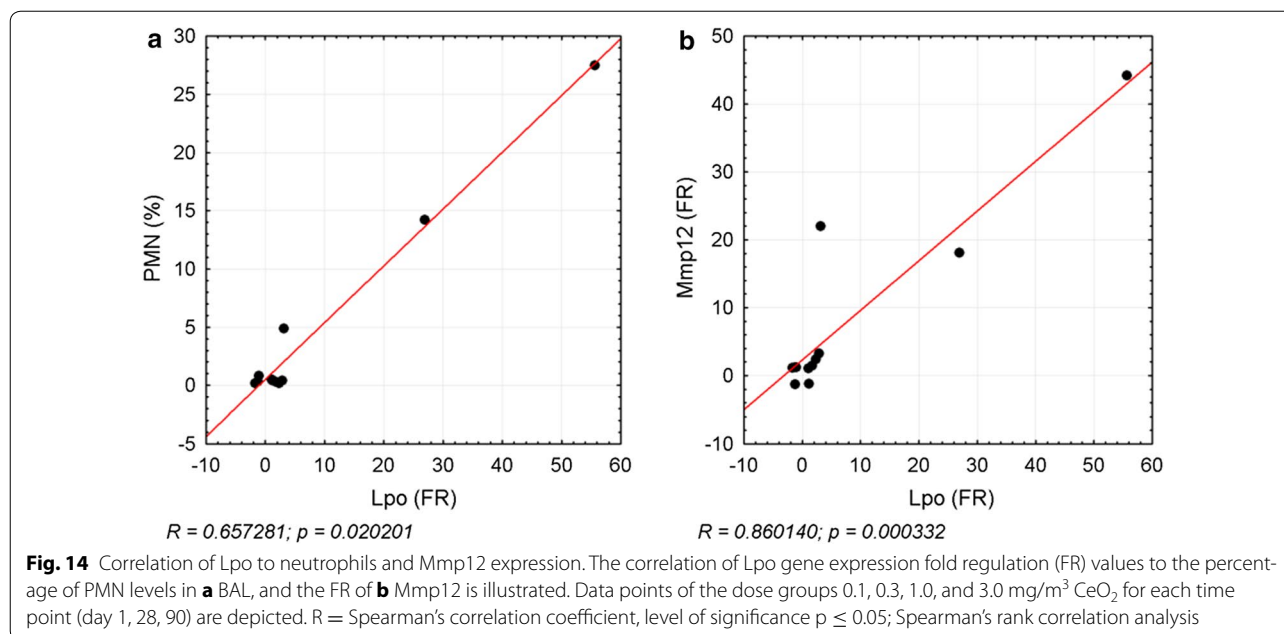


**Table 4** Amounts of Ce in liver and kidney tissue after CeO<sub>2</sub> nanoparticle exposure

Dose group	Ce	Ce content (µg/organ ± SD)				
		Day 1	Days 28	Days 90 + 1	Days 90 + 28	Days 90 + 90
4 (liver)	Ionic	0.025 ± 0.001	0.27 ± 0.068**	0.717 ± 0.407**	0.68 ± 0.38**	0.46 ± 0.70**
	Particulate	0.054 ± 0.001	0.081 ± 0.04**	1.308 ± 1.094**	1.13 ± 1.58**	0.42 ± 0.24*
	Total	0.079 ± 0.002	0.34 ± 0.049**	2.025 ± 1.182**	1.81 ± 1.78**	0.88 ± 0.60*
5 (liver)	Ionic	< 0.025	0.35 ± 0.038**	1.30 ± 0.45**	1.03 ± 0.43**	1.26 ± 1.13**
	Particulate	< 0.025	0.13 ± 0.080	1.65 ± 3.00*	1.40 ± 1.61**	0.54 ± 0.31**
	Total	< 0.025	0.48 ± 0.078**	2.95 ± 3.04**	2.43 ± 1.50**	1.45 ± 0.85**
4 (kidney)	Ionic	0.11 ± 0.06	0.11 ± 0.07	0.04 ± 0.01	0.04 ± 0.01	0.05 ± 0.03
	Particulate	0.04 ± 0.03	0.07 ± 0.03	0.15 ± 0.10*	0.07 ± 0.02	0.05 ± 0.02
	Total	0.15 ± 0.07	0.18 ± 0.10	0.19 ± 0.09	0.11 ± 0.02	0.09 ± 0.05
5 (kidney)	Ionic	0.018 ± 0.001	0.025 ± 0.000	0.032 ± 0.012**	0.041 ± 0.009**	0.059 ± 0.015**
	Particulate	0.025 ± 0.010	0.021 ± 0.006	0.030 ± 0.003	0.033 ± 0.029	0.042 ± 0.02
	Total	0.029 ± 0.011	0.033 ± 0.018	0.050 ± 0.019	0.073 ± 0.033*	0.084 ± 0.038*

Dose groups: 4 = 1.0 mg/m<sup>3</sup> CeO<sub>2</sub>, 5 = 3.0 mg/m<sup>3</sup> CeO<sub>2</sub>; Values are expressed as mean ± SD, \* p < 0.05, \*\* p < 0.01 vs. d 1, n ≤ 5; Kruskal–Wallis–ANOVA with Mann–Whitney U-test as post hoc analysis; detection limit for analysis of liver tissue: 0.025 µg; detection limit for analysis of kidney tissue: 0.015 µg





the NANoREG long-term study performed by BASF (81|0661/10|170). We measured effects less severe compared to CeO<sub>2</sub>, despite the at least 16-fold higher concentration, which supports the low effect hypothesis. However, some unexpected findings in BaSO<sub>4</sub> exposed lungs have been detected and need to be evaluated.

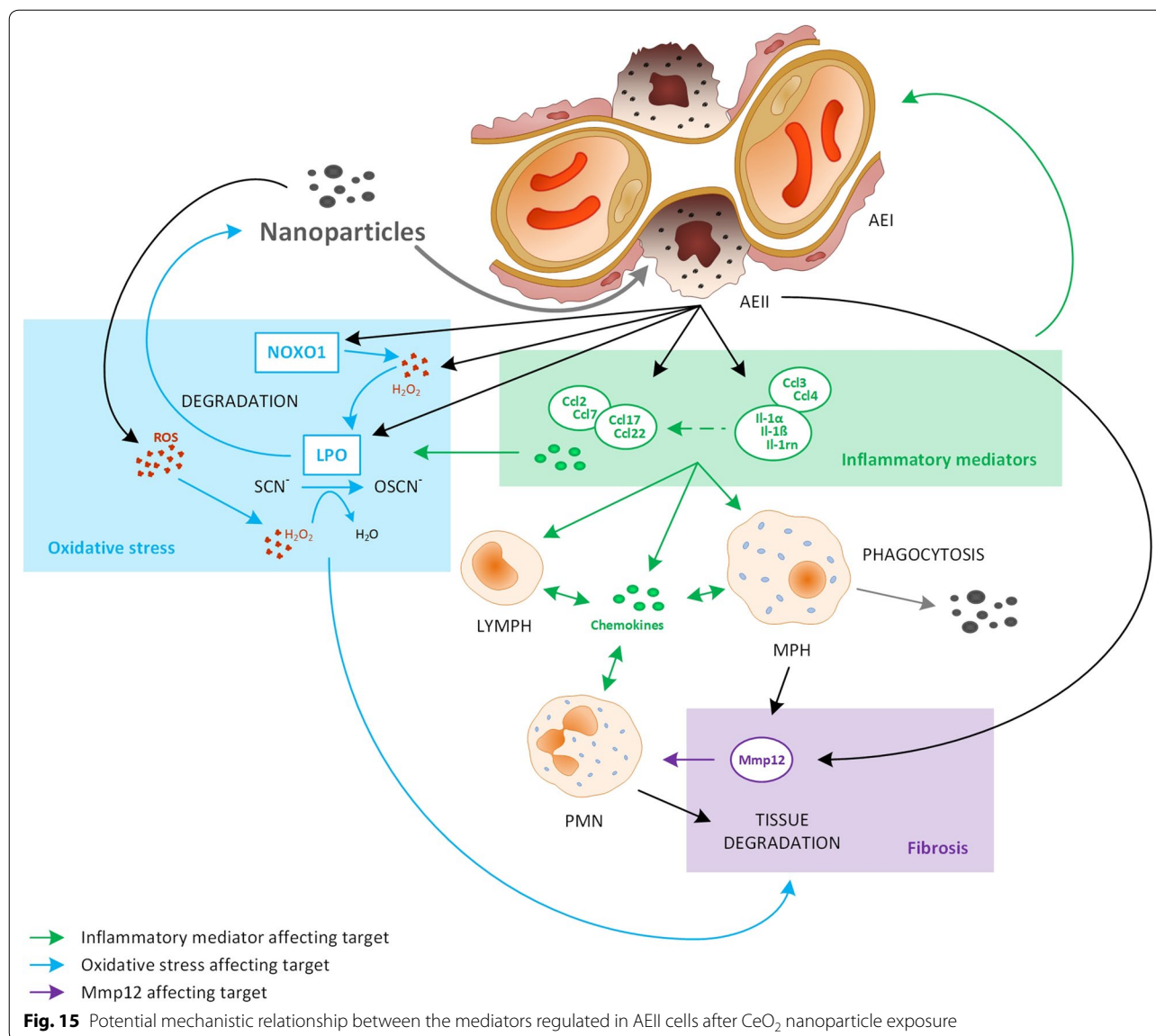
Pulmonary inflammation and some changes in AEII cell gene expression levels were measured. Major histopathological findings in the nasal cavity with minor inflammation of the alveolar compartment were attributed to particle deposition favoring the upper respiratory tract rather than the alveoli because of high particle accumulation [1]. This might be the reason for the lower impact on gene regulation in AEII cells compared to CeO<sub>2</sub>.

Interestingly, the majority of genes affected by BaSO<sub>4</sub> were also affected by CeO<sub>2</sub>. Similar to CeO<sub>2</sub> the highest response in the group of inflammatory mediators was measured for the C–C-motif chemokine Ccl22. In vitro data on the influence of BaSO<sub>4</sub> on macrophages or neutrophils regarding expression of inflammatory mediators and cell migration did not show activation of respective mechanisms [71, 72]. Particles like silica and TiO<sub>2</sub> in contrast, had stimulating effects [72]. All in all, the impact of BaSO<sub>4</sub> on inflammatory mediator release compared to CeO<sub>2</sub> is rather low. Post-exposure decrease of Ccl2 protein levels in BAL supported by decreases in severity of histopathological findings after the end of 90 days exposure [1] further suggest reversibility of the inflammatory reaction.

Although BaSO<sub>4</sub> NM-220 was demonstrated to bear no intrinsic oxidative potential [73], the oxidative stress marker Lpo was highly upregulated. Like for CeO<sub>2</sub> a marked increase of Lpo protein in AEII cells was identified in areas of inflammation. This verifies a mechanistic relationship between the particle-induced inflammation and oxidative stress. Further, the quantification of the Lpo signal displayed a lower, but significant elevation in comparison to CeO<sub>2</sub>.

Signs for genotoxicity and apoptosis were minimal, but a strong effect of BaSO<sub>4</sub> nanoparticle exposure on Mmp12 was detected. Considering the relation of Mmp12 to chronic pulmonary effects like fibrosis, potential adverse reactions due to long-term BaSO<sub>4</sub> become more likely. However, such findings were not detected in previous histopathological investigations [1]. Also, Mmp12 protein levels in lung tissue remain unaffected. Since Mmp12 further indicates inflammation, the elevated gene expression levels in AEII cells detected for BaSO<sub>4</sub> might be related to the inflammatory reaction without notifying chronic adverse effects.

Although BaSO<sub>4</sub> was cleared from the respiratory tract quite rapid and no overload situation was provoked during 90-day particle exposure [1], the very high amount of particles entering the respiratory tract might be a reason for detection of unexpected effects like increased Lpo, Ccl22 or Mmp12. The phenomenon of fast clearance was pointed out in our previous research [1]. The dissolution of BaSO<sub>4</sub> nanoparticles is assumed to be generally low. However, according to Konduru et al. [74], who stated a



dissolution rate of < 1% in different media, the fast clearance could be attributed to changes in the dissolution rate because of e.g. switches in surface charge of the nanoparticles. Nevertheless an explicit reason for the phenomenon of fast BaSO<sub>4</sub> clearance remains unknown and needs to be further investigated. Our results further show that CeO<sub>2</sub> and BaSO<sub>4</sub> caused similar responses in AEII cells while the response pattern still allowed differentiation between both substances. The higher inflammatory potential of CeO<sub>2</sub> was appropriately reflected. Mediators displaying quite high responses (Lpo, Ccl22, Mmp12) might be suitable markers for nanomaterial toxicity testing. To further clarify the specific function of Lpo or Mmp12 as response to CeO<sub>2</sub> and BaSO<sub>4</sub> nanoparticles,

investigations of the respective markers after exposure to other nanoparticles with a known oxidative, genotoxic or tumorigenic potential are needed.

#### Systemic effects of CeO<sub>2</sub> and BaSO<sub>4</sub> nanoparticles on liver and kidney tissue

Nanomaterial generally bears a certain potential to translocate to extra-pulmonary organs after inhalation and organs responsible for excretion are common targets. We investigated gene expression in liver and kidney tissue after 90 days exposure. The number of regulated genes was lower compared to AEII cells with less overlap between pulmonary and extra-pulmonary compartments. Distribution of genes over the different pathways

however was similar especially in liver tissue where effects on inflammatory mediators were dominating. Interestingly in the kidney a great portion of genes associated with oxidative stress were downregulated. CeO<sub>2</sub> had a higher impact than BaSO<sub>4</sub> on both organs.

It has been demonstrated by Aalapati et al. [19] that a small fraction of CeO<sub>2</sub> nanoparticles accumulate in liver and kidney and cause histopathological changes after inhalation in mice. The kidney was assumed to be the major extra-pulmonary target organ for nanoparticles. Nemmar et al. [30] comprehensively investigated inflammation, oxidative stress and DNA damage in extrapulmonary tissues after CeO<sub>2</sub> intratracheal instillation and reported adverse findings for all endpoints in liver and kidney.

Our findings show upregulation of different C-X-C motif chemokines and receptors responsible for neutrophil recruitment in liver tissue in response to CeO<sub>2</sub>, indicating inflammatory reactions. In kidney tissue almost all genes affected by CeO<sub>2</sub> displayed downregulation, therefore suggesting a rather anti-inflammatory and anti-oxidative effect in this organ. Since potential effects of CeO<sub>2</sub> are controversial and positive health effects have been described [75], a positive impact of translocating particles to the kidneys could be conceivable.

As basis for discussion of the present findings, we exemplarily determined the level of Ce in liver and kidney tissue during and after nanoparticle exposure to the higher concentrations. We found a small amount of ionic and particulate Ce in the liver, showing an expected development of increase during and decrease after exposure. In the previous study we measured peak levels of 1300 µg Ce retained per lung [1]. This amount derived from a concentration of 3.0 mg/m<sup>3</sup> CeO<sub>2</sub> NM-212 administered over 90 days (6 h/day, 5 days/week) at a deposition fraction of 9.6%. In the liver we found 3 µg/organ at these conditions. The fraction translocated to the liver from the amount present in the lung was thus 0.23%. However, the increase of Ce levels is significant over time and a contribution to the changes in gene expression is conceivable. It also needs to be considered that modulated gene expression can be caused by other systemically distributed mediators as a response to the present lung inflammation. Also the Ce level was slightly lower after 1.0 mg/m<sup>3</sup> CeO<sub>2</sub> exposure compared to 3.0 mg/m<sup>3</sup> CeO<sub>2</sub>. This indicates a concentration-dependency which has clearly been detected in the lung as well [1]. Even lower levels are thus assumed for the lower dose groups. At earlier stages of exposure the amount of ionic Ce was higher than the particulate proportion. This indicates that translocation of particles occurs with delay due to barriers and defense mechanisms. As described earlier CeO<sub>2</sub>

nanoparticles likely influence the cellular balance of ROS due to redox activity. This ability is contributed to ion formation on the nanoparticle surface [75]. The amount of ionic Ce could be a result of this ion formation. The high Lpo levels detected in this study indicate oxidative stress in the lung. The amount of ionic Ce in this tissue however, was negligible [1]. The ion content could therefore not be correlated to the level of oxidative stress. In liver and kidney tissue the overall modulation of gene regulation was too low to adequately assess a potential correlation between ion formation and oxidative stress in these organs. The effects on gene expression and the amount of Ce in extra-pulmonary organs was overall very low. The question in how far these findings contribute to potential adverse effects thus remains unanswered. No significant increases of Ce levels were detected in kidney tissue. It could be assumed that the downregulation of several genes was rather caused by other signals, like endogenous mediators, than the nanoparticles. Due to the low response to BaSO<sub>4</sub> in terms of gene expression after 90 days and the less clear results for CeO<sub>2</sub> we did not include barium retention in our investigations at this point.

## Conclusion

Our results suggest that CeO<sub>2</sub> related lung inflammation was supported by chemokine release of AEII cells and characterized by increased monocyte activation with subsequent neutrophil and lymphocyte infiltrations. Stimulation of rat AEII cells is likely not exclusively overload but also substance related. At low concentrations it is dominated by interleukins like IL-1α, IL-1β and chemokine expression. With increasing concentrations and induction of lung overload gene regulation exacerbates and the chemokine pattern switches. AEII cells further respond with signs of oxidative stress indicated by increased Lpo and Nox1 in the presences of CeO<sub>2</sub> and the mediators can be considered as potential early marker for nanoparticle oxidative stress induction after inhalation. Genes related to genotoxicity and apoptosis were not markedly affected by CeO<sub>2</sub> exposure. However, due to the upregulation of Mmp12 a relation to potential long-term effects like fibrosis and lung cancer could be assumed. Respective findings need to be related to the long-term inhalation toxicity study (BASE, Ludwigshafen, Germany) to further support significance.

BaSO<sub>4</sub> nanoparticle exposure has a rather low influence on the expression of inflammatory mediators in AEII cells. However, we detected some changes in gene regulation, which supports the assumption that the nanomaterial affects the organism after inhalation although it is considered as chemically inert. Interestingly, mediators

like Lpo, Ccl22 and Mmp12, highly affected by CeO<sub>2</sub> exposure also responded to BaSO<sub>4</sub>. Such mediators are promising biomarkers for nanomaterial toxicity testing.

The overall effect on gene expression in liver and kidney was low. However, especially in the liver some inflammatory mediators were upregulated. Also, low but significant Ce levels were present in the liver. A contribution of the particles to changes in gene expression of extra-pulmonary organs therefore still needs to be taken into consideration and further research should focus on this issue.

## Methods

### Test substances

The test materials cerium dioxide NM-212 and barium sulfate NM-220 belong to the Nanomaterial Repository of the European Commission Joint Research Center (JRC, Ispra, Italy) and were provided by the Fraunhofer Institute for Molecular Biology and Applied Ecology (Schmalenberg, Germany).

### Animals

For this study female Wistar rats [CrI:WI (Han)] at the age of 10 weeks during start of exposure were used (Charles River, Sulzfeld, Germany). Beforehand, animals were acclimatized to laboratory conditions for 1 week, trained for restraint in nose-only tubes over 3 weeks and were randomly distributed to control and treatment groups, respectively. The following conditions were set for animal housing: 20–24 °C, 40–70% relative humidity, 12 h light/dark cycle. Laboratory diet (“V1534”, sniff Spezialdiaeten GmbH, Soest, Germany) and water was supplied ad libitum. All experiments and animal handling was conducted in compliance with the Regulations of the German Animal Protection Law (Tierschutzgesetz of May 18, 2006).

### Nose-only inhalation

The examinations described here were performed as additional part to the conventional investigation of a 90-day inhalation toxicity study according to OECD TG 413. For gene expression analysis, 90 animals were exposed to clean air or the test substances via nose-only inhalation for one, 28 and 90 days in concentrations of 0.1, 0.3, 1.0 and 3.0 mg/m<sup>3</sup> for CeO<sub>2</sub> nanoparticles and 50.0 mg/m<sup>3</sup> for BaSO<sub>4</sub> nanoparticles (5 rats/dose group/time point). Aerosol generation was done via dry powder dispersion using a dispersion nozzle developed at Fraunhofer ITEM and the respective aerosol generation system [76]. Aerosol concentrations were constantly checked via an aerosol photometer (Fraunhofer ITEM, Hannover, Germany). The MMAD of the samples was determined by gravimetry (Marple 298 Personal Cascade Impactor,

Thermo Fisher Scientific, Dreieich, Germany). Animals were kept in the inhalation system 5 days a week for 6 h each day. They were checked for clinical signs daily before and after exposure. Bodyweight as well as food and water consumption was recorded weekly.

### Gene expression analysis

#### *Alveolar epithelial type II cell isolation and organ extraction*

After one, 28 and 90 days of exposure to either clean air, the different CeO<sub>2</sub> NM-212 concentrations or BaSO<sub>4</sub> NM-220, rat lungs were prepared on the following day for isolation of AEII cells and subsequent gene expression analysis. The method of AEII isolation is based on the work of Richards et al. [77] and Dobbs et al. [78] and well established in our institute [79]. We further performed comprehensive methodical research on this topic in mice [80]. Minor modifications on the current protocol have been taken for the work with rats. Briefly, animals were anesthetized (Ketamine/Xylazine, 10:1; bela-pharm, Vechta, Germany/Bayer, Leverkusen, Germany) via intraperitoneal injection. For lung perfusion, the trachea was uncovered and cut to introduce a cannula for artificial ventilation. Abdominal cavity and thorax were opened and a cannula was inserted via the vena cava inferior into the right ventricle. Pulmonary perfusion was done with PBS (5 mL/min, 25 mL Biochrom, Berlin, Germany) and a peristaltic pump while the lung was constantly manually ventilated. An incision in the left atrium served as perfusate outflow. Finally, the lung was explanted for subsequent tissue digestion and cell isolation. During sacrifice the caudate lobe of the liver as well as the right kidney were removed and stored at – 80 °C for RNA isolation. The isolated lung was flushed with PBS, treated with dispase (Sigma-Aldrich, Taufkirchen, Germany) and manually dissected. Respective steps were followed by DNase digestion (Sigma-Aldrich, Taufkirchen, Germany) and passage through two nylon sieves with different mesh size (250, 60 μM). After several steps of centrifugation IgG panning (Sigma-Aldrich, Taufkirchen, Germany) was performed to remove unwanted cell types, including macrophages. One hour incubation was followed by another DNase digestion. Finally, the isolated cells were separated by centrifugation and the pellet was stored at – 80 °C for RNA isolation. AEII cell extraction from rat lungs yielded  $5.3 \pm 2.5 \times 10^6$  cells per individual which was sufficient for subsequent processing.

#### *RNA Isolation*

RNA isolation from AEII cells, liver and kidney tissue was performed using the RNeasy Mini Kit (QIAGEN, Hilden, Germany) according to the manufacturer's instructions including a DNase treatment procedure (RNase-Free DNase Set, QIAGEN, Hilden, Germany).

RNA extraction and subsequent gene expression analysis was done for AEII cells after one, 28 and 90 days of nanoparticle exposure (90 samples in total). For liver and kidney tissues 90-day exposure samples were processed (in total 30 samples each). Amount and quality of RNA were measured with the NanoDrop ND-1000 Spectrophotometer, Version 3.7 (Thermo Fisher Scientific, Dreieich, Germany) and the Agilent 2100 Bioanalyzer (Agilent Technologies, Ratingen, Germany), respectively. The amount of RNA extracted from liver tissue was highest ( $78.4 \pm 21.3 \mu\text{g}$ ), followed by kidney ( $45.2 \pm 6.5 \mu\text{g}$ ) and AEII cells ( $15.6 \pm 5.6 \mu\text{g}$ ). Measurements of RNA quality yielded mean RNA integrity numbers (RIN)  $> 7.0$  for liver, kidney and AEII cells, respectively, indicating RNA samples of good quality.

### **RT<sup>2</sup> profiler PCR arrays**

To screen a broad spectrum of potential effects of nanoparticle exposure, the following RT<sup>2</sup> profiler PCR arrays (SABiosciences/QIAGEN, Hilden, Germany) were applied for AEII samples: inflammatory cytokines and receptors (PARN-011Z), oxidative stress (PARN-065Z), DNA repair (PARN-042Z), apoptosis (PARN-012Z), lung cancer (PARN-134Z). For RNA isolated from liver and kidney the same arrays were used except of the lung cancer array. The commercially available arrays contain qPCR assays for the analysis of 84 different genes related to the respective end points in a 96 well format (84 genes, 5 potential reference genes, 7 quality controls). The quality controls consist of a genomic DNA contamination control (1 $\times$ ), a reverse transcription efficiency control (3 $\times$ ) and a PCR efficiency control (3 $\times$ ). For the present study we created customized arrays, by pooling four commercial arrays in a 384 well format. The fifth array was spotted four times on a 384 well plate for simultaneous analysis of four samples. Some genes are overlapping between the pathways and therefore in total 391 different genes were analyzed per AEII RNA sample and 325 genes per RNA sample extracted from liver and kidney tissues (Additional file 2: Table S2). In a first step, cDNA synthesis was performed using the RT<sup>2</sup> First Strand Kit (SABiosciences/QIAGEN, Hilden, Germany), following the manufacturer's instructions. Subsequently, RT<sup>2</sup> Profiler PCR arrays were conducted according to the manufacturer's instructions using the real-time PCR system ViiA<sup>TM</sup>7 (Applied Biosystems/Thermo Fisher Scientific Inc., Dreieich, Germany). An amount of 1.19 ng was applied per single RTqPCR assay.

### **Data evaluation**

Data analysis of exported "Cycle Threshold" ( $C_T$ ) values was performed based on the comparative  $\Delta\Delta C_T$  method described by Schmittgen and Livak [81], using the

provided SABiosciences PCR Array Data Analysis Template Excel<sup>®</sup> and web-based software (SABiosciences/QIAGEN, Hilden, Germany; <https://www.qiagen.com/de/products/genes%20and%20pathways/data-analysis-center-overview-page/?UID=70f8b4af-789d-4788-af6f-b12ebd800888#>). One to three stable expressed reference genes were chosen for each time point and tissue for normalization using NormFinder [82] and geNorm algorithm [83] as part of the GenEx Professional 6 Software (bioMCC, Freising, Germany). The fold regulation (FR) values generated for each gene describe the factor of up- or downregulation in a certain treatment group related versus the control group. Genes displaying FR values  $\leq -2$  or  $\geq 2$  were considered as relevant. Genes with high  $C_T$  values ( $\geq 35$ ) or abnormal melting curves were excluded. Statistical significance of FR values was checked with Student's *T* test ( $p \leq 0.05$ ).  $C_T$  values, if normal distributed, were further checked for outliers within the group of five animals for each experimental condition and gene, according to Grubbs [84]. Respective values were eliminated if necessary, FR values were recalculated and statistical significance testing was repeated as described above. Genes with FR values  $\leq -2$  or  $\geq 2$  were selected for further analysis concerning function and relevance in the context of the study focus, independent of their statistical significance. Already changes in individual animals are important, because a completely identical genetic background of the animals should not reasonably be assumed.

Correlation analysis was performed using fold regulation (FR) values (gene expression data) or mean percentages (BAL data, main study) of all CeO<sub>2</sub> dose groups and time points for the two compared variables. Data were correlated using Spearman rank correlation analysis ( $p \leq 0.05$ ).

### **Cytokine levels in bronchoalveolar lavage**

Levels of the cytokines Ccl2, Ccl20, Il-1 $\alpha$ , and Il-1 $\beta$  were measured in bronchoalveolar lavages (BAL) of rat lungs after one and 28 days as well as one, 28 and 90 days post-90-day exposure to clean air, the different CeO<sub>2</sub> NM-212 concentrations or BaSO<sub>4</sub> NM-220. BAL was performed according to Henderson et al. [85] with minor modifications. Lungs were lavaged twice using 4 mL 0.9% NaCl. For cytokine analysis 1 mL of the BAL fluid was removed. Cytokine levels were determined using a MULTI-SPOT<sup>®</sup> 4 Spot Cytokine Custom Rat 4-Plex kit for the four analytes (Meso Scale Discovery, Rockville, USA), according to the manufacturer's instructions.

### **Immunohistochemistry**

For immunohistological analysis, two consecutive lung tissue sections were prepared. Examinations were done

in rats exposed to either clean air, 3.0 mg/m<sup>3</sup> CeO<sub>2</sub> NM-212 or 50.0 mg/m<sup>3</sup> BaSO<sub>4</sub> NM-220 for one, 28 or 90 days. Lungs were fixed in 10% formalin and trimmed based on the work of Kittel et al. [86]. To detect the presence of lactoperoxidase (Lpo, rabbit polyclonal, Acris, NBP1-87010) and matrixmetalloproteinase 12 (Mmp12, rabbit polyclonal, Abcam, ab66157) antibodies directed against those markers were applied as described by Rittinghausen et al. [87]. Immunohistochemically stained lung sections were counterstained with hematoxylin and digitalized using slide scanner (MiraxScanner, Zeiss, Germany) and quantified using image analyzing software (ZeissZen, Zeiss, Germany). Quantified Lpo and Mmp12 levels were statistically evaluated using Kruskal–Wallis–ANOVA with Mann–Whitney U-test as post hoc analysis.

### Retention analytics

Cerium contents were measured in liver and kidney tissue of five animals of the mid and high dose group after one and 28 exposure days and one, 28 and 90 days post-90-day exposure. The isotopes <sup>140</sup>Ce/<sup>142</sup>Ce were quantified via inductively coupled plasma mass spectrometry (ICP-MS) using a quadrupole ICP-MS system (X-Serie II, Thermo Fisher Scientific). The shredded tissue was lyophilized for at least 6 h (0.37 mbar). Prior and subsequently to freeze-drying organ weights were recorded. Plasma ashing (cool plasma conditions, 400 W, 1 mbar O<sub>2</sub>, 24 h) and subsequent microwave digestion (H<sub>2</sub>SO<sub>4</sub>, 96%, supra quality, max. 500 W) was performed to further remove organic material. To distinguish between CeO<sub>2</sub> particles and soluble CeO<sub>2</sub> a semiquantitative technique was implemented using nuclear pore filters (diameter: 0.1 μm).

### Additional files

**Additional file 1: Table S1.** Fold regulation of regulated genes. List of fold regulation and standard deviation values of the regulated genes listed in Tables 2 and 3 of the manuscript. Values are shown for every dose group and time point.

**Additional file 2: Table S2.** Analyzed genes per array. List of all analyzed genes (short and long name) separated per PCR profiler array.

### Abbreviations

8-OHdG: 8-oxo-2'-deoxyguanosine; AEI cells: alveolar epithelial cells type I; AEII cells: alveolar epithelial cells type II; Alb: albumin; BAL: bronchoalveolar lavage; Birc5: baculoviral IAP repeat-containing 5; Brca1: breast cancer 1; Ccl11: C–C motif chemokine ligand 11; Ccl17: C–C motif chemokine ligand 17; Ccl2: C–C motif chemokine ligand 2; Ccl20: C–C motif chemokine ligand 20; Ccl22: C–C motif chemokine ligand 22; Ccl24: C–C motif chemokine ligand 24; Ccl3: C–C motif chemokine ligand 3; Ccl4: C–C motif chemokine ligand 4; Ccl7: C–C motif chemokine ligand 7; Ccl9: chemokine (C–C motif) ligand 9; Ccr2: chemokine (C–C motif) receptor 2; Cd40lg: CD40 ligand; COPD: chronic obstructive lung disease; Cx3cl1: chemokine (C–X3–C motif) ligand 1; Cx3cr1: C–X3–C motif chemokine receptor 1; Cxcl12: chemokine (C–X–C motif) ligand

12; Cxcl9: C–X–C motif chemokine ligand 9; Cxcr2: chemokine (C–X–C motif) receptor 2; Cxcr3: chemokine (C–X–C motif) receptor 3; Cxcr5: chemokine (C–X–C motif) receptor 5; Cyp1b1: cytochrome P450, family 1, subfamily b, polypeptide 1; Epx: eosinophil peroxidase; Exo1: exonuclease 1; Fabp4: fatty acid binding protein 4; FR: fold regulation; Gcll: glutamate-cysteine ligase, catalytic SU; Gclm: glutamate cysteine ligase, modifier SU; Gpx2: glutathione peroxidase 2; Hba1: hemoglobin alpha, adult chain 2; IFNγ: interferon gamma; Il1rn: interleukin 1 receptor antagonist; Il1α: interleukin 1 alpha; Il1β: interleukin 1 beta; Il2rb: interleukin 2 receptor, beta; Il2rg: interleukin 2 receptor, gamma; Krt1: keratin 1; LDH: lactate dehydrogenase; Lig4: ligase IV, DNA, ATP-dependent; Lpo: lactoperoxidase; LYMPH: lymphocyte; Mmp12: matrix metalloproteinase 12; MPH: macrophage; Mpo: myeloperoxidase; Msh5: mutS homolog 5; Mutyh: MutY homolog (*E. coli*); NADPH: nicotinamide adenine dinucleotide phosphate; Ncf2: neutrophil cytosolic factor 2; Ngb: neuroglobin; Noxo1: NADPH oxidase organizer 1; OECD: Organization for Economic Co-operation and Development; Opcml: opioid binding protein/cell adhesion molecule-like; Osm: oncostatin M; Pf4: Platelet factor 4; PMN: polymorphonuclear neutrophil; ROS: reactive oxygen species; Scd1: stearyl-Coenzyme A desaturase 1; Smug1: single-strand-selective monofunctional uracil-DNA glycosylase 1; SOD: superoxide dismutase; Spp1: secreted phosphoprotein 1; SWCNT: single walled carbon nanotubes; Tcf21: transcription factor 21; Thbs2: thrombospondin 2; Tnfsf4: tumor necrosis factor superfamily member 4; Top2a: topoisomerase (DNA) II alpha; Txnip: thioredoxin interacting protein; Xrcc2: X-ray repair complementing defective repair in Chinese hamster cells 2; γ-H2AX: histon γ-H2AX.

### Authors' contributions

DS was responsible for study planning and management. She was further involved in laboratory work including animal exposure, AEII cell isolation and gene expression analysis. She processed all gene expression data, performed statistical evaluations and wrote major parts of the manuscript. MN reviewed gene expression analyses and highly contributed to manuscript writing with valuable scientific and structural input. DS performed immunohistochemical tissue staining and analysis, provided the photographs and was involved in interpretation and discussion of immunohistochemical data. HK performed chemical analytics of the substances and was involved in retention data analysis. TH supervised AEII cell isolation and contributed to manuscript reviewing. CD initiated and supervised the study and importantly contributed to manuscript reviewing. OC was involved in project initiation and management as well as interpretation and discussion of results. All authors read and approved the final manuscript.

### Acknowledgements

The authors thank all other employees of Fraunhofer ITEM, involved in the project for excellent technical assistance and intellectual input. Special thanks to Janosch Kretzschmann for creative support and critical review of the overview figure.

### Competing interests

The authors declare that they have no competing interests.

### Availability of data and materials

The datasets generated and analyzed during the current study are available from the corresponding author on reasonable request.

### Consent for publication

Not applicable.

### Ethics approval and consent to participate

All experiments were conducted and approved according to the German Animal Welfare Act by the local authority at the LAVES Niedersachsen, Hannover, Germany, No. 33.12-42502-04-14/1564.

### Funding

All experiments were funded by the German Federal Ministry of Education and Research (BMBF) within the project InHaIT-90: "90 days inhalation testing with CeO<sub>2</sub> in the rat and subsequent analysis of gene expression profiles for the early detection of toxic/carcinogenic effects" (tag: 03X0149).

## Publisher's Note

Springer Nature remains neutral with regard to jurisdictional claims in published maps and institutional affiliations.

Received: 21 December 2017 Accepted: 13 February 2018

Published online: 20 February 2018

## References

- Schwotzer D, Ernst H, Schaudien D, Kock H, Pohlmann G, Dasenbrock C, Creutzenberg O. Effects from a 90-day inhalation toxicity study with cerium oxide and barium sulfate nanoparticles in rats. *Part Fibre Toxicol*. 2017;14:23. <https://doi.org/10.1186/s12989-017-0204-6>.
- Pison U, Max M, Neuendank A, Weißbach S, Pietschmann S. Host defence capacities of pulmonary surfactant: evidence for 'non-surfactant' functions of the surfactant system. *Eur J Clin Invest*. 1994;24:586–99.
- Paine R, Rolfe MW, Standiford TJ, Burdick MD, Rollins BJ, Strieter RM. MCP-1 expression by rat type II alveolar epithelial cells in primary culture. *J Immunol*. 1993;150:4561–70.
- Standiford TJ, Kunkel SL, Phan SH, Rollins BJ, Strieter RM. Alveolar macrophage-derived cytokines induce monocyte chemoattractant protein-1 expression from human pulmonary type II-like epithelial cells. *J Biol Chem*. 1991;266:9912–8. <https://doi.org/10.2165/00128413-199107860-00011>.
- van Berlo D, Knaapen AM, van Schooten F-J, Schins RP, Albrecht C. NF-kappaB dependent and independent mechanisms of quartz-induced proinflammatory activation of lung epithelial cells. *Part Fibre Toxicol*. 2010;7:13. <https://doi.org/10.1186/1743-8977-7-13>.
- Driscoll KE, Howard BW, Carter JM, Asquith T, Johnston C, Detilleux P, et al. Alpha-quartz-Induced chemokine expression by rat lung epithelial cells. *Am J Pathol*. 1996;149:1627–37.
- Barlow PG, Clouter-Baker A, Donaldson K, Maccallum J, Stone V. Carbon black nanoparticles induce type II epithelial cells to release chemotaxins for alveolar macrophages. *Part Fibre Toxicol*. 2005;2:11. <https://doi.org/10.1186/1743-8977-2-11>.
- Chen S, Yin R, Mutze K, Yu Y, Takenaka S, Königshoff M, Stoeger T. No involvement of alveolar macrophages in the initiation of carbon nanoparticle induced acute lung inflammation in mice. *Part Fibre Toxicol*. 2016;13:33. <https://doi.org/10.1186/s12989-016-0144-6>.
- Kuhn DA, Vanhecke D, Michen B, Blank F, Gehr P, Petri-Fink A, Rothen-Rutishauser B. Different endocytotic uptake mechanisms for nanoparticles in epithelial cells and macrophages. *Beilstein J Nanotechnol*. 2014;5:1625–36. <https://doi.org/10.3762/bjnano.5.174>.
- Thorley AJ, Ruenaroengsak P, Potter TE, Tetley TD. Critical determinants of uptake and translocation of nanoparticles by the human pulmonary alveolar epithelium. *ACS Nano*. 2014;8:11778–89. <https://doi.org/10.1021/nr505399e>.
- Kemp SJ, Thorley AJ, Gorelik J, Seckl MJ, O'Hare MJ, Arcaro A, et al. Immortalization of human alveolar epithelial cells to investigate nanoparticle uptake. *Am J Respir Cell Mol Biol*. 2008;39:591–7. <https://doi.org/10.1165/rcmb.2007-0334OC>.
- Schumann C, Schubbe S, Cavelius C, Kraegeloh A. A correlative approach at characterizing nanoparticle mobility and interactions after cellular uptake. *J Biophotonics*. 2012;5:117–27. <https://doi.org/10.1002/jbio.201100064>.
- Schaudien D, Knebel J, Creutzenberg O. In vitro study revealed different size behavior of different nanoparticles. *J Nanopart Res*. 2012;14:593. <https://doi.org/10.1007/s11051-012-1039-6>.
- Geiser M, Quail O, Wenk A, Wigge C, Eigeldinger-Berthou S, Hirn S, et al. Cellular uptake and localization of inhaled gold nanoparticles in lungs of mice with chronic obstructive pulmonary disease. *Part Fibre Toxicol*. 2013;10:19. <https://doi.org/10.1186/1743-8977-10-19>.
- Conhaim RL, Dovi WF, Watson KE, Spiegel CA, Harms BA. Bacteremia does not affect cellular uptake of ultrafine particles in the lungs of rats. *Anat Rec (Hoboken)*. 2011;294:550–7. <https://doi.org/10.1002/ar.21326>.
- Ma J, Bishoff B, Mercer RR, Barger M, Schwegler-Berry D, Castranova V. Role of epithelial–mesenchymal transition (EMT) and fibroblast function in cerium oxide nanoparticles-induced lung fibrosis. *Toxicol Appl Pharmacol*. 2017;323:16–25. <https://doi.org/10.1016/j.taap.2017.03.015>.
- Oberdörster G. Lung particle overload: implications for occupational exposure to particles. *Regul Toxicol Pharmacol*. 1995;27:123–35.
- Schins RPF. Mechanisms of genotoxicity of particles and fibers. *Inhal Toxicol*. 2002;14:57–78. <https://doi.org/10.1080/089583701753338631>.
- Aalapati S, Ganapathy S, Manapuram S, Anumolu G, Prakya BM. Toxicity and bio-accumulation of inhaled cerium oxide nanoparticles in CD1 mice. *Nanotoxicology*. 2014;8:786–98. <https://doi.org/10.3109/17435390.2013.829877>.
- Demokritou P, Gass S, Pyrgiotakis G, Cohen JM, Goldsmith W, McKinney W, et al. An in vivo and in vitro toxicological characterisation of realistic nanoscale CeO(2) inhalation exposures. *Nanotoxicology*. 2013;7:1338–50. <https://doi.org/10.3109/17435390.2012.739665>.
- Gosens I, Mathijssen LE, Bokkers BGH, Muijsers H, Cassee FR. Comparative hazard identification of nano- and micro-sized cerium oxide particles based on 28-day inhalation studies in rats. *Nanotoxicology*. 2014;8:643–53. <https://doi.org/10.3109/17435390.2013.815814>.
- Keller J, Wohleben W, Ma-Hock L, Strauss V, Groters S, Kuttler K, et al. Time course of lung retention and toxicity of inhaled particles: short-term exposure to nano-ceria. *Arch Toxicol*. 2014;88:2033–59. <https://doi.org/10.1007/s00204-014-1349-9>.
- Landsiedel R, Ma-Hock L, Hofmann T, Wiemann M, Strauss V, Treumann S, et al. Application of short-term inhalation studies to assess the inhalation toxicity of nanomaterials. *Part Fibre Toxicol*. 2014;11:16. <https://doi.org/10.1186/1743-8977-11-16>.
- Larsen ST, Jackson P, Poulsen SS, Levin M, Jensen KA, Wallin H, et al. Airway irritation, inflammation, and toxicity in mice following inhalation of metal oxide nanoparticles. *Nanotoxicology*. 2016;10:1254–62. <https://doi.org/10.1080/17435390.2016.1202350>.
- Morimoto Y, Izumi H, Yoshiura Y, Tomonaga T, Oyabu T, Myojo T, et al. Pulmonary toxicity of well-dispersed cerium oxide nanoparticles following intratracheal instillation and inhalation. *J Nanopart Res*. 2015;17:442. <https://doi.org/10.1007/s11051-015-3249-1>.
- Srinivas A, Rao PJ, Selvam G, Murthy PB, Reddy PN. Acute inhalation toxicity of cerium oxide nanoparticles in rats. *Toxicol Lett*. 2011;205:105–15. <https://doi.org/10.1016/j.toxlet.2011.05.1027>.
- Eom H-J, Choi J. Oxidative stress of CeO<sub>2</sub> nanoparticles via p38-Nrf-2 signaling pathway in human bronchial epithelial cell, beas-2B. *Toxicol Lett*. 2009;187:77–83. <https://doi.org/10.1016/j.toxlet.2009.01.028>.
- Lin W, Huang Y-W, Zhou X-D, Ma Y. Toxicity of cerium oxide nanoparticles in human lung cancer cells. *Int J Toxicol*. 2006;25:451–7. <https://doi.org/10.1080/10915810600959543>.
- Mittal S, Pandey AK. Cerium oxide nanoparticles induced toxicity in human lung cells: role of ROS mediated DNA damage and apoptosis. *Biomed Res Int*. 2014;2014:891934. <https://doi.org/10.1155/2014/891934>.
- Nemmar A, Yuvaraju P, Beegam S, Fahim MA, Ali BH. Cerium oxide nanoparticles in lung acutely induce oxidative stress, inflammation, and DNA damage in various organs of mice. *Oxid Med Cell Longev*. 2017;2017:9639035. <https://doi.org/10.1155/2017/9639035>.
- Rubio L, Annangi B, Vila L, Hernandez A, Marcos R. Antioxidant and anti-genotoxic properties of cerium oxide nanoparticles in a pulmonary-like cell system. *Arch Toxicol*. 2016;90:269–78. <https://doi.org/10.1007/s00204-015-1468-y>.
- Xia T, Kovoichich M, Liong M, Madler L, Gilbert B, Shi H, et al. Comparison of the mechanism of toxicity of zinc oxide and cerium oxide nanoparticles based on dissolution and oxidative stress properties. *ACS Nano*. 2008;2:2121–34. <https://doi.org/10.1021/nr800511k>.
- Kumari M, Kumari SI, Grover P. Genotoxicity analysis of cerium oxide micro and nanoparticles in Wistar rats after 28 days of repeated oral administration. *Mutagenesis*. 2014;29:467–79. <https://doi.org/10.1093/mutage/geu038>.
- Kumari M, Kumari SI, Kamal SSK, Grover P. Genotoxicity assessment of cerium oxide nanoparticles in female Wistar rats after acute oral exposure. *Mutat Res Genet Toxicol Environ Mutagen*. 2014;775–776:7–19. <https://doi.org/10.1016/j.mrgentox.2014.09.009>.
- El Yamani N, Collins AR, Runden-Pran E, Fjellsbo LM, Shaposhnikov S, Zielondiny S, Dusinska M. In vitro genotoxicity testing of four reference metal nanomaterials, titanium dioxide, zinc oxide, cerium oxide and silver: towards reliable hazard assessment. *Mutagenesis*. 2017;32:117–26. <https://doi.org/10.1093/mutage/gew060>.
- Cordelli E, Keller J, Eleuteri P, Villani P, Ma-Hock L, Schulz M, et al. No genotoxicity in rat blood cells upon 3- or 6-month inhalation exposure

- to CeO<sub>2</sub> or BaSO<sub>4</sub> nanomaterials. *Mutagenesis*. 2016. <https://doi.org/10.1093/mutage/gew005>.
37. Ma JY, Mercer RR, Barger M, Schwegler-Berry D, Scabillon J, Ma JK, Castranova V. Induction of pulmonary fibrosis by cerium oxide nanoparticles. *Toxicol Appl Pharmacol*. 2012;262:255–64. <https://doi.org/10.1016/j.taap.2012.05.005>.
  38. Ma JYC, Young S-H, Mercer RR, Barger M, Schwegler-Berry D, Ma JK, Castranova V. Interactive effects of cerium oxide and diesel exhaust nanoparticles on inducing pulmonary fibrosis. *Toxicol Appl Pharmacol*. 2014;278:135–47. <https://doi.org/10.1016/j.taap.2014.04.019>.
  39. Geraets L, Oomen AG, Schroeter JD, Coleman VA, Cassee FR. Tissue distribution of inhaled micro- and nano-sized cerium oxide particles in rats: results from a 28-day exposure study. *Toxicol Sci*. 2012;127:463–73. <https://doi.org/10.1093/toxsci/kfs113>.
  40. He X, Zhang H, Ma Y, Bai W, Zhang Z, Lu K, et al. Lung deposition and extrapulmonary translocation of nano-ceria after intratracheal instillation. *Nanotechnology*. 2010;21:285103. <https://doi.org/10.1088/0957-4484/21/28/285103>.
  41. Li D, Morishita M, Wagner JG, Fatouraie M, Wooldridge M, Eagle WE, et al. In vivo biodistribution and physiologically based pharmacokinetic modeling of inhaled fresh and aged cerium oxide nanoparticles in rats. *Part Fibre Toxicol*. 2016;13:45. <https://doi.org/10.1186/s12989-016-0156-2>.
  42. Molina RM, Konduru NV, Jimenez RJ, Pyrgiotakis G, Demokritou P, Wohlleben W, Brain JD. Bioavailability, distribution and clearance of tracheally instilled, gavaged or injected cerium dioxide nanoparticles and ionic cerium. *Environ Sci Nano*. 2014;1:561–73. <https://doi.org/10.1039/C4EN00034J>.
  43. Nalabotu SK, Kolli MB, Triest WE, Ma JY, Manne Nandini D P K, Katta A, et al. Intratracheal instillation of cerium oxide nanoparticles induces hepatic toxicity in male Sprague–Dawley rats. *Int J Nanomed*. 2011;6:2327–35. <https://doi.org/10.2147/IJN.S25119>.
  44. Proost P, Wuyts A, van Damme J. Human monocyte chemotactic proteins-2 and -3: structural and functional comparison with MCP-1. *J Leukoc Biol*. 1996;59:67–74.
  45. Nakanishi T, Imaizumi K, Hasegawa Y, Kawabe T, Hashimoto N, Okamoto M, Shimokata K. Expression of macrophage-derived chemokine (MDC)/CCL22 in human lung cancer. *Cancer Immunol Immunother*. 2006;55:1320–9. <https://doi.org/10.1007/s00262-006-0133-y>.
  46. Imai T, Nagira M, Takagi S, Kakizaki M, Nishimura M, Wang J, et al. Selective recruitment of CCR4-bearing Th2 cells toward antigen-presenting cells by the CC chemokines thymus and activation-regulated chemokine and macrophage-derived chemokine. *Int Immunol*. 1999;11:81–8. <https://doi.org/10.1093/intimm/11.1.81>.
  47. Neagos J, Standiford TJ, Newstead MW, Zeng X, Huang SK, Ballinger MN. Epigenetic regulation of tolerance to toll-like receptor ligands in alveolar epithelial cells. *Am J Respir Cell Mol Biol*. 2015;53:872–81. <https://doi.org/10.1165/rcmb.2015-00570C>.
  48. Bello-Irizarry SN, Wang J, Olsen K, Gigliotti F, Wright TW. The alveolar epithelial cell chemokine response to pneumocystis requires adaptor molecule MyD88 and interleukin-1 receptor but not toll-like receptor 2 or 4. *Infect Immun*. 2012;80:3912–20. <https://doi.org/10.1128/IAI.00708-12>.
  49. Chuquimia OD, Petrusdottir DH, Rahman MJ, Hartl K, Singh M, Fernandez C. The role of alveolar epithelial cells in initiating and shaping pulmonary immune responses: communication between innate and adaptive immune systems. *PLoS ONE*. 2012;7:e32125. <https://doi.org/10.1371/journal.pone.0032125>.
  50. Wang J, Gigliotti F, Bhagwat SP, Maggirwar SB, Wright TW. Pneumocystis stimulates MCP-1 production by alveolar epithelial cells through a JNK-dependent mechanism. *Am J Physiol Lung Cell Mol Physiol*. 2007;292:L1495–505. <https://doi.org/10.1152/ajplung.00452.2006>.
  51. Manzer R, Wang J, Nishina K, McConville G, Mason RJ. Alveolar epithelial cells secrete chemokines in response to IL-1β and lipopolysaccharide but not to ozone. *Am J Respir Cell Mol Biol*. 2006;34:158–66. <https://doi.org/10.1165/rcmb.2005-0205OC>.
  52. Christensen PJ, Du M, Moore B, Morris S, Toews GB, Paine R. Expression and functional implications of CCR2 expression on murine alveolar epithelial cells. *Am J Physiol Lung Cell Mol Physiol*. 2004;286:L68–72. <https://doi.org/10.1152/ajplung.00079.2003>.
  53. Barrett EG, Johnston C, Oberdörster G, Finkelstein JN. Silica-induced chemokine expression in alveolar type II cells is mediated by TNF-α. *Am J Physiol Lung Cell Mol Physiol*. 1998;275:1110–9.
  54. Tao F, Kobzik L. Lung macrophage–epithelial cell interactions amplify particle-mediated cytokine release. *Am J Respir Cell Mol Biol*. 2002;26:499–505. <https://doi.org/10.1165/ajrcmb.26.4.4749>.
  55. Driscoll KE. Macrophage inflammatory proteins: biology and role in pulmonary inflammation. *Exp Lung Res*. 1994;20:473–90. <https://doi.org/10.3109/01902149409031733>.
  56. O'Brien AD, Standiford TJ, Christensen PJ, Wilcoxon SE, Paine R. Chemotaxis of alveolar macrophages in response to signals derived from alveolar epithelial cells. *J Lab Clin Med*. 1998;131:417–24. [https://doi.org/10.1016/S0022-2143\(98\)90142-1](https://doi.org/10.1016/S0022-2143(98)90142-1).
  57. Brabcová E, Kolesár L, Thorburn E, Strž I. Chemokines induced in human respiratory epithelial cells by IL-1 family of cytokines. *Folia Biol*. 2014;60:180–6.
  58. McIntyre BAS, Kushwah R, Mechael R, Shapovalova Z, Alev C, Bhatia M. Innate immune response of human pluripotent stem cell-derived airway epithelium. *Innate Immun*. 2015;21:504–11. <https://doi.org/10.1177/1753425914551074>.
  59. Finkelstein JN, Johnston C, Barrett T, Oberdörster G. Particulate-cell interactions and pulmonary cytokine expression. *Environ Health Perspect*. 1997;105:1179–82. <https://doi.org/10.1289/ehp.97105s51179>.
  60. Gattas MV, Forteza R, Fragoso MA, Fregien N, Salas P, Salathe M, Conner GE. Oxidative epithelial host defense is regulated by infectious and inflammatory stimuli. *Free Radic Biol Med*. 2009;47:1450–8. <https://doi.org/10.1016/j.freeradbiomed.2009.08.017>.
  61. Bhattacharya K, El-Sayed R, Andón FT, Mukherjee SP, Gregory J, Li H, et al. Lactoperoxidase-mediated degradation of single-walled carbon nanotubes in the presence of pulmonary surfactant. *Carbon*. 2015;91:506–17. <https://doi.org/10.1016/j.carbon.2015.05.022>.
  62. Hoffstein ST, Gennaro DE, Manzi RM. Neutrophils may directly synthesize both H<sub>2</sub>O<sub>2</sub> and O<sub>2</sub>—since surface stimuli induce their release in stimulus-specific ratios. *Inflammation*. 1985;9:425–37.
  63. Fischer H. Mechanisms and function of DUOX in epithelia of the lung. *Antioxid Redox Signal*. 2009;11:2453–65. <https://doi.org/10.1089/ars.2009.2558>.
  64. Brandes RP, Weissmann N, Schröder K. Nox family NADPH oxidases: molecular mechanisms of activation. *Free Radic Biol Med*. 2014;76:208–26. <https://doi.org/10.1016/j.freeradbiomed.2014.07.046>.
  65. van Klaveren RJ, Roelant C, Boogaerts M, Demedts M, Nemery B. Involvement of an NAD(P)H oxidase-like enzyme in superoxide anion and hydrogen peroxide generation by rat type II cells. *Thorax*. 1997;52:465–71.
  66. Nénan S, Boichot E, Lagente V, Bertrand CP. Macrophage elastase (MMP-12): a pro-inflammatory mediator? *Mem Inst Oswaldo Cruz*. 2005;100(1):167–72.
  67. Lagente V, Manoury B, Nénan S, Le Quément C, Martin-Chouly C, Boichot E. Role of matrix metalloproteinases in the development of airway inflammation and remodeling. *Braz J Med Biol Res*. 2005;38:1521–30. <https://doi.org/10.1590/S0100-879X2005001000009>.
  68. Park E-J, Yoon J, Choi K, Yi J, Park K. Induction of chronic inflammation in mice treated with titanium dioxide nanoparticles by intratracheal instillation. *Toxicology*. 2009;260:37–46. <https://doi.org/10.1016/j.tox.2009.03.005>.
  69. Shukla A, Barrett TF, Nakayama KI, Nakayama K, Mossman BT, Lounsbury KM. Transcriptional up-regulation of MMP12 and MMP13 by asbestos occurs via a PKCδ-dependent pathway in murine lung. *FASEB J*. 2006;20:997–9. <https://doi.org/10.1096/fj.05-4554fj>.
  70. Conner GE, Wijkstrom-Frei C, Randell SH, Fernandez VE, Salathe M. The lactoperoxidase system links anion transport to host defense in cystic fibrosis. *FEBS Lett*. 2007;581:271–8.
  71. Loza K, Fohring I, Bunger J, Westphal GA, Koller M, Epple M, Sengstock C. Barium sulfate micro- and nanoparticles as bioinert reference material in particle toxicology. *Nanotoxicology*. 2016. <https://doi.org/10.1080/17435390.2016.1235740>.
  72. Schremmer I, Brik A, Weber DG, Rosenkranz N, Rostek A, Loza K, et al. Kinetics of chemotaxis, cytokine, and chemokine release of NR8383 macrophages after exposure to inflammatory and inert granular insoluble particles. *Toxicol Lett*. 2016;263:68–75. <https://doi.org/10.1016/j.toxlet.2016.08.014>.
  73. Delaval M, Wohlleben W, Landsiedel R, Baeza-Squiban A, Boland S. Assessment of the oxidative potential of nanoparticles by the cytochrome c assay: assay improvement and development of a

- high-throughput method to predict the toxicity of nanoparticles. *Arch Toxicol*. 2017;91:163–77. <https://doi.org/10.1007/s00204-016-1701-3>.
74. Konduru N, Keller J, Ma-Hock L, Groters S, Landsiedel R, Donaghey TC, et al. Biokinetics and effects of barium sulfate nanoparticles. *Part Fibre Toxicol*. 2014;11:55. <https://doi.org/10.1186/s12989-014-0055-3>.
  75. Celardo I, Pedersen JZ, Traversa E, Ghibelli L. Pharmacological potential of cerium oxide nanoparticles. *Nanoscale*. 2011;3:1411–20. <https://doi.org/10.1039/c0nr00875c>.
  76. Koch W. Application of aerosols. In: Uhlig S, Taylor AE, editors. *Methods in pulmonary research*. Basel: Birkhäuser Basel; 1998. p. 485–507. [https://doi.org/10.1007/978-3-0348-8855-4\\_19](https://doi.org/10.1007/978-3-0348-8855-4_19).
  77. Richards RJ, Davies N, Atkins J, Oreffo VIC. Isolation, biochemical characterization, and culture of lung type II cells of the rat. *Lung*. 1987;165:143–58. <https://doi.org/10.1007/BF02714430>.
  78. Dobbs LG, Gonzalez R, Williams MC. An improved method for isolating type II cells in high yield and purity. *Am Rev Respir Dis*. 1986;134:141–5.
  79. Hansen T, Blickweide M, Borlak J. Primary rat alveolar epithelial cells for use in biotransformation and toxicity studies. *Toxicol In Vitro*. 2006;20:757–66. <https://doi.org/10.1016/j.tiv.2005.10.011>.
  80. Hansen T, Chougule A, Borlak J. Isolation and cultivation of metabolically competent alveolar epithelial cells from A/J mice. *Toxicol In Vitro*. 2014;28:812–21. <https://doi.org/10.1016/j.tiv.2014.03.009>.
  81. Schmittgen TD, Livak KJ. Analyzing real-time PCR data by the comparative CT method. *Nat Protoc*. 2008;3:1101–8. <https://doi.org/10.1038/nprot.2008.73>.
  82. Andersen CL, Jensen JL, Ørntoft TF. Normalization of real-time quantitative reverse transcription-PCR data: a model-based variance estimation approach to identify genes suited for normalization, applied to bladder and colon cancer data sets. *Cancer Res*. 2004;64:5245–50. <https://doi.org/10.1158/0008-5472.CAN-04-0496>.
  83. Vandesompele J, de Preter K, Pattyn F, Poppe B, van Roy N, de Paepe A, Speleman F. Accurate normalization of real-time quantitative RT-PCR data by geometric averaging of multiple internal control genes. *Genome Biol*. 2002;3:1–11. <https://doi.org/10.1186/gb-2002-3-7-research0034>.
  84. Grubbs FE. Procedures for detecting outlying observations in samples. *Technometrics*. 1969;11:1–21. <https://doi.org/10.1080/00401706.1969.10490657>.
  85. Henderson RF, Mauderly JL, Pickrell JA, Hahn FF, Muhle H, Rebar AH. Comparative study of bronchoalveolar lavage fluid: effect of species, age, and method of lavage. *Exp Lung Res*. 1987;13:329–42. <https://doi.org/10.3109/01902148709069597>.
  86. Kittel B, Ruehl-Fehlert C, Morawietz G, Klapwijk J, Elwell MR, Lenz B, et al. Revised guides for organ sampling and trimming in rats and mice—part 2. A joint publication of the RITA and NACAD groups. *Exp Toxicol Pathol*. 2004;55:413–31.
  87. Rittinghausen S, Bellmann B, Creutzenberg O, Ernst H, Kolling A, Mangelsdorf I, et al. Evaluation of immunohistochemical markers to detect the genotoxic mode of action of fine and ultrafine dusts in rat lungs. *Toxicology*. 2013;303:177–86. <https://doi.org/10.1016/j.tox.2012.11.007>.

Submit your next manuscript to BioMed Central and we will help you at every step:

- We accept pre-submission inquiries
- Our selector tool helps you to find the most relevant journal
- We provide round the clock customer support
- Convenient online submission
- Thorough peer review
- Inclusion in PubMed and all major indexing services
- Maximum visibility for your research

Submit your manuscript at  
[www.biomedcentral.com/submit](http://www.biomedcentral.com/submit)

